Annual Review of Fluid Mechanics

FLEET Velocimetry for Aerodynamics

Paul M. Danehy,[1] Ross A. Burns,[2] Daniel T. Reese,[1] Jonathan E. Retter,[2] and Sean P. Kearney[3]

[1]NASA Langley Research Center, Hampton, Virginia, USA; email: paul.m.danehy@nasa.gov

[2]National Institute of Aerospace, Hampton, Virginia, USA

[3]Sandia National Laboratories, Albuquerque, New Mexico, USA

Annu. Rev. Fluid Mech. 2022. 54:525–53

The *Annual Review of Fluid Mechanics* is online at fluid.annualreviews.org

https://doi.org/10.1146/annurev-fluid-032321-025544

Keywords

flow velocimetry, molecular tagging, experimental fluid mechanics, ultrafast diagnostics, wind tunnel testing, femtosecond excitation

Abstract

Long-lasting emission from femtosecond excitation of nitrogen-based flows shows promise as a useful mechanism for a molecular tagging velocimetry instrument. The technique, known as femtosecond laser electronic excitation tagging (FLEET), was invented at Princeton a decade ago and has quickly been adopted and used in a variety of high-speed ground test flow facilities. The short temporal scales offered by femtosecond amplifiers permit nonresonant multiphoton excitation, dissociation, and weak ionization of a gaseous medium near the beam's focus without the generation of a laser spark observed with nanosecond systems. Gated, intensified imaging of the resulting emission enables the tracking of tagged molecules, thereby measuring one to three components of velocity. Effects of local heating and acoustic disturbances can be mitigated with the selection of a shorter-wavelength excitation source. This review surveys the development of FLEET over the decade since its inception, as it has been implemented in several test facilities to make accurate, precise, and seedless velocimetry measurements for studying complex high-speed flows.

1. INTRODUCTION

CFD: computational fluid dynamics

MTV: molecular tagging velocimetry

LDV: laser Doppler velocimetry

DGV: Doppler global velocimetry

PIV: particle image velocimetry

PTV: particle tracking velocimetry

Velocity measurement techniques are critical for understanding fluid flow over or through complex configurations, with the aerodynamics community holding particular interest in the development of such techniques for the purposes of design and research. Modern-day aerodynamic testing combines design informed by computational fluid dynamics (CFD) with experimental validation in suitable ground test facilities (Georgiadis et al. 2014, Slotnick et al. 2014, Clark et al. 2020). Typically, the greatest CFD uncertainties arise in the most challenging fluid environments, such as near-surface boundary layer profiles or flow separation on smooth walls or in wakes. On-body techniques coupled with force balance measurements are routine in wind tunnel facilities but remain inadequate to properly evaluate and validate fluid models, which encourages the continued development of off-body flow techniques. Unfortunately, many large-scale ground test facilities were constructed before the advent of laser-based diagnostics for fluid flow measurements. Thus, current-day implementation of such tools remains a challenge on many practical levels (engineering challenges, optical access, vibrations, etc.).

There remains a need for accurate off-body velocimetry measurements in ground test facilities, where the degree of implementation of laser diagnostics has been dependent on the facility. Particle-based methods are now widely used in subsonic to mildly supersonic flow facilities, and initial molecular tagging velocimetry (MTV) techniques have shown promise for high-speed benchtop flows but generally remain too complex for large-scale implementation except in rare circumstances. However, the recent introduction of femtosecond lasers as a means to tag nitrogen-based flow fields, named femtosecond laser electronic excitation tagging (FLEET) (Michael et al. 2011, Miles et al. 2018), has provided a useful and comparatively simple MTV method for accurate flow velocimetry. **Figure 1** highlights the advancement of FLEET over the course of a decade, from velocity profiles in benchtop free jets (Michael et al. 2011) to applications in a variety of wind tunnels (Burns & Danehy 2017; Dogariu et al. 2019; Reese et al. 2019b, 2021). These examples and others are discussed in this practical review of the FLEET technique, with an emphasis placed on its use in large-scale wind tunnel facilities for aerodynamic testing.

1.1. Particle-Based Velocimetry

One of the earliest and most widely used solutions for measuring flow velocity in aerodynamic ground test facilities was seeding the flow with small particles that act as flow tracers, where the measured particle velocity was related back to the actual flow itself. These techniques replaced physical probes in many cases and originated with laser Doppler velocimetry (LDV) instruments for point measurements, which have now expanded to various forms of Doppler global velocimetry (DGV) (Cadel & Lowe 2015) and particle image velocimetry (PIV) or particle tracking velocimetry (PTV) instruments (Adrian 1991, Westerweel et al. 2013) for measurements of two or three components of velocity at a point, in a plane, or in a volume. These are now standard tools in the engineering community, with corresponding commercial and open-source software to transform the imaged Mie scattered light into velocity vectors.

However, the inherent drawback with particle-based techniques is the difficulty in seeding the flow with particles, as well as the fact that the particles themselves can alter the flow field or can provide only a measure of particle velocity and not the desired flow velocity. There are many options for seeding (Melling 1997), and care must be taken to ensure the proper seeding is chosen for each application to best approximate the fluid of interest. For high-speed flows, accurate particle drag relations (Loth 2008) are required to infer the fluid response from the measured particle response, particularly flow through shockwaves (Williams et al. 2015). Finally, from a practical perspective, not all test facilities allow for particle seeding due to the possible

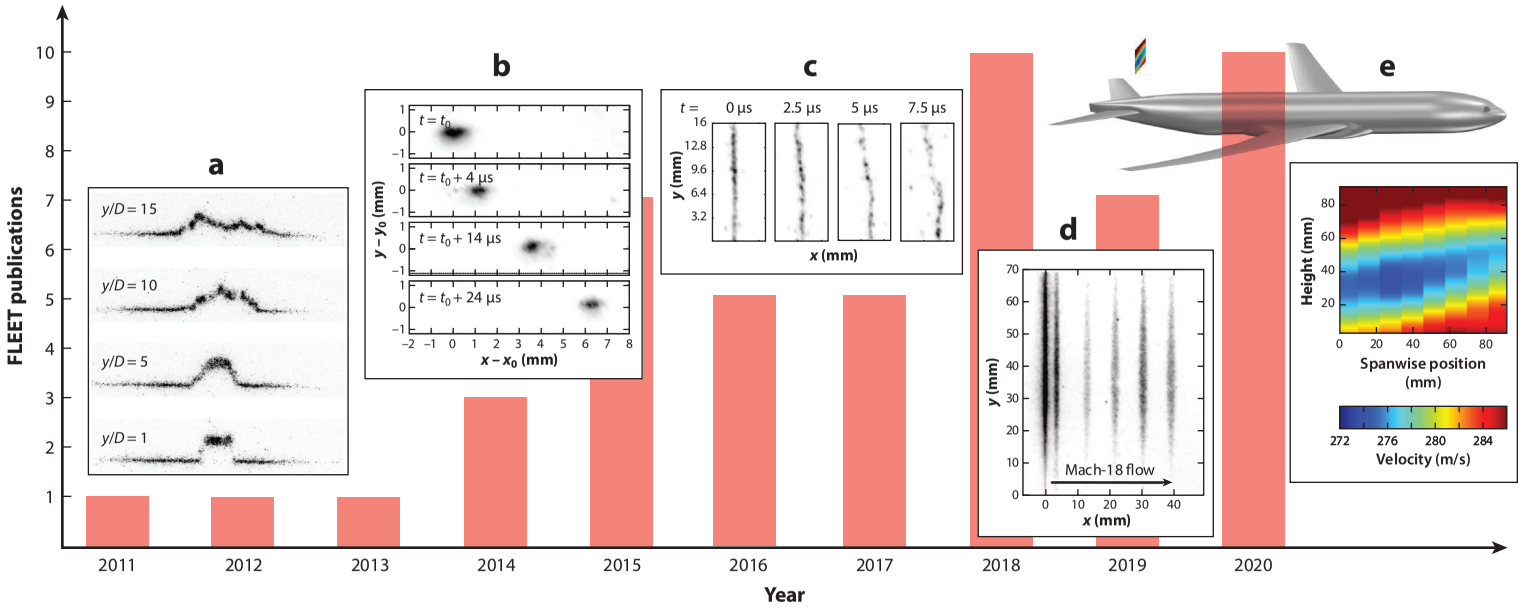

Figure 1

Published uses of FLEET velocimetry over time, highlighting (*a*) the original FLEET work in a free jet; (*b*) point measurements in the 0.3-m Transonic Cryogenic Tunnel at the NASA Langley Research Center; (*c*) raw STARFLEET (selective two-photon absorptive resonance FLEET) images in the wake of a cylinder model in a Mach-8 flow, with the flow direction from left to right; (*d*) representative freestream images in a Mach-18 flow; and (*e*) velocity profiles from the wake of the common research model in the NASA Langley Research Center's National Transonic Facility. Panels adapted with permission from (*a*) Michael et al. (2011), (*b*) Burns & Danehy (2017), (*c*) Reese et al. (2019b), (*d*) Dogariu et al. (2021), and (*e*) Reese et al. (2021).

contamination of the model or the facility itself (Fisher et al. 2021), leaving the investigator with only particle-free options for velocimetry.

1.2. Particle-Free Velocimetry

The development of particle-free techniques has received the most significant interest in high-speed flow environments (Miles & Lempert 1997) to overcome the limitations of particle-based methods. These particle-free methods are based on either Doppler shift detection or molecular tagging. Filtered Rayleigh scattering is one such Doppler shift technique, where the velocity is inferred by imaging the intensity of Doppler-shifted Rayleigh–Brillouin scattering through a narrow-band filter such as a molecular iodine cell (i.e., the seed-free version of DGV). For a fixed experimental setup and known gas parameters (temperature, pressure, and species), one can directly infer the velocity. However, in practice, the thermodynamic state is not known and a scanning approach is required to simultaneously fit all parameters in the gas phase (Forkey et al. 1996, Boguszko & Elliott 2005, Doll et al. 2017), providing an average measure of the gas velocity and thermodynamic properties over a measurement plane. Similar time- or space-averaged approaches include laser-induced fluorescence (LIF) (McDaniel et al. 1983, Klavuhn et al. 1994, Danehy et al. 2001) and tunable diode laser absorption spectroscopy (Hanson 2011) techniques, respectively. These methods scan over an absorption line and measure the Doppler shift of the absorption profile.

An alternative class of particle-free measurements tag molecules in a fluid, typically by resonant laser excitation to an excited state or by photo-dissociation of a target species, and track the average displacement of the resulting photon emission during the decay or recombination from the tagged molecules in the flow between successive detector exposures. As summarized in **Table 1** and reviewed elsewhere (Koochesfahani & Nocera 2007), there is a variety of these MTV techniques targeting energy levels in specific molecules. These methods are attractive in high-speed flows, as MTV techniques do not suffer from particle lag, as illustrated by Huffman & Elliott (2009) in an MTV and PIV comparison across a Mach disk from a free jet.

Table 1 Overview of MTV techniques

Technique	Media	Excitation wavelengths	Reference(s)
RELIEF	O_2	Three colors (Raman pair + UV)	Miles et al. 1987
APART	O_2	Three colors (UV + UV)	Sijtsema et al. 2002
VENOM	NO_2	Three colors (V + UV)	Sánchez-González et al. 2011
OTV	O_3	Three colors (UV + UV)	Pitz et al. 2000
HTV	OH	Three colors (UV + UV)	Ribarov et al. 2002
PHANTOMM	PAFs	Three colors (UV + V)	Lempert et al. 1995
KTV	Kr	Three colors (UV + V)	Mills et al. 2011, Parziale et al. 2015
Biacetyl MTV	Biacetyl	One color (V)	Hiller et al. 1984
Acetone MTV	Acetone	One color (UV)	Lempert et al. 2002
LIF	NO, I_2	One color (UV)	Danehy et al. 2003, Balla 2013
FLEET	N_2	One color (UV to NIR)[a]	Michael et al. 2011

Abbreviations: APART, air photolysis and recombination tracking; FLEET, femtosecond laser electronic excitation tagging; HTV, hydroxyl tagging velocimetry; KTV, krypton tagging velocimetry; LIF, laser-induced fluorescence; MTV, molecular tagging velocimetry; NIR, near-infrared; OTV, ozone tagging velocimetry; PAFs, photo-activated fluorophores; PHANTOMM, photo-activated nonintrusive tracking of molecular motion; RELIEF, Raman excitation plus laser-induced electronic fluorescence; UV, ultraviolet; V, visible; VENOM, vibrationally excited NO monitoring.

[a]Demonstrated thus far: 1,064, 800, 400, 267, 202.25, and 202 nm.

However, not all MTV techniques are easy to implement, as most are resonant approaches targeting specific molecular energy levels, thereby requiring the coinciding tunable, and usually ultraviolet (UV), laser hardware to produce the specified frequencies, which increases the complexity of the experimental setup. Sometimes multiples of such laser systems are required. Others require seeding the fluorescing species into the flow globally or locally if not naturally present, altering the composition of the test medium and possibly changing the natural flow pattern itself. These mechanical and optical complexities combined with the challenging environments imposed by large-scale ground test facilities have largely precluded the use of molecular tagging techniques for practical engineering measurements. The advent of FLEET velocimetry saw many of these issues addressed simultaneously.

FLEET (Michael et al. 2011) provides an easy-to-implement yet robust form of molecular tagging. **Table 1** highlights the major benefits of FLEET in comparison to other techniques. First, inert nitrogen gas (N_2) is prevalent in many fluid/combustion systems and at times is the only gas present in ground test facilities (Goodyer 1992, Beresh et al. 2015, Dogariu et al. 2019, Fisher et al. 2021); therefore, no foreign gas seeding is required. Second, FLEET is a nonresonant multiphoton process; therefore, only a single ultrafast laser source is required to produce a FLEET signal over a variety of excitation wavelengths, avoiding the need to frequency-tune the fundamental output of a laser system. The use of a single-laser, single-camera velocimetry instrument greatly simplifies experimental setup and data acquisition, making FLEET an attractive velocimetry tool for a variety of flow facilities. While FLEET has already been a component of a few review articles on ultrafast diagnostics (Miles et al. 2015, Li et al. 2018), this review focuses exclusively on FLEET velocimetry and closely related methods, detailing the underlying mechanism, a variety of experimental configurations, and a series of recent impactful ground testing results.

2. EXCITATION AND EMISSION MECHANISM

2.1. Overview

FLEET is performed by tracking in time the fluorescence of nitrogen excited by intense, focused femtosecond laser pulses. This fluorescence is occasionally referred to as a filament, generated by the forced self-focusing of a pulse with a convex lens, but the exact FLEET line formation mechanism remains up for debate. The physical process is hypothesized to occur in three phases: (*a*) the dissociation, ionization, and electronic excitation of nitrogen molecules by multiple incoming photons; (*b*) the delayed recombination of dissociated nitrogen atoms into high-lying electronic energy levels of N_2; and (*c*) the emission of photons from these states, which returns the molecules to the ground electronic state. The long-lasting (tens of microseconds) FLEET signal is predominantly from photon emission from the *B* to *A* states observed in the yellow-orange-red region of the visible spectrum. Molecules undergoing such a process are known as the tagged species. Discussions of the underlying mechanisms are found in many FLEET-based sources (DeLuca et al. 2014, Zhang 2018, Li et al. 2019, Peters 2019), as well as earlier fundamental femtosecond filament work unrelated to the measure of flow velocity (Chin 2009, Xu et al. 2009). Here we present an overview.

Most experimental fluid dynamicists are probably more familiar with nanosecond laser-induced breakdown, where a violent spark is formed at the laser focus. A femtosecond breakdown is fundamentally different due to the $\sim 10^6$ shorter timescale of the energy deposition. The differences are depicted in **Figure 2** and have been highlighted by Talebpour et al. (2001), Limbach (2015), and Hsu et al. (2018b). **Figure 2** depicts multiphoton ionization and dissociation that occur immediately after the onset of a high-energy laser pulse (either femtosecond or nanosecond) tightly focused in N_2. For a nanosecond pulse, the gaseous medium undergoes multiphoton ionization to

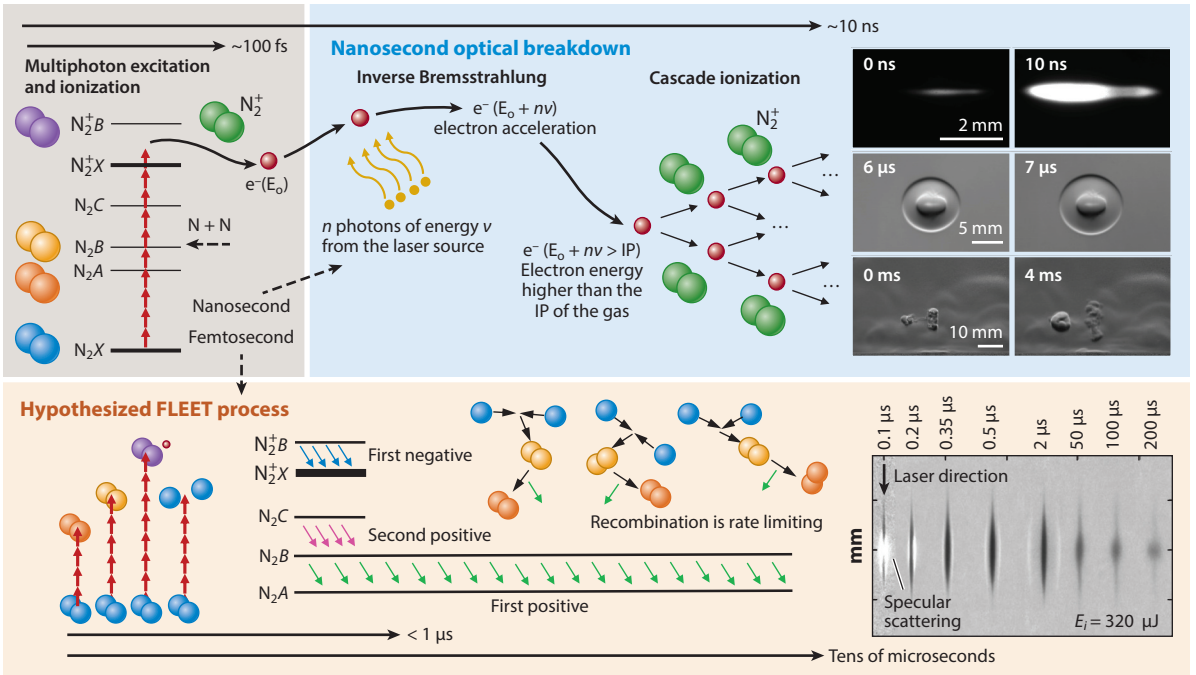

Figure 2

Illustration of the nanosecond (*top row*; *blue*) and femtosecond (*bottom row*; *orange*) interactions of a laser pulse with nitrogen gas (N_2). The long temporal duration of nanosecond pulses permits the interaction of free electrons with ongoing electromagnetic radiation (ν), leading to increased electron energies (E_o) through the absorption of n photons during inverse Bremsstrahlung processes and the eventual cascade ionization of the gaseous medium when the electron energy is elevated above the gas ionization potential (IP). The top right corner shows emission imaging (*top row*) and schlieren imaging (*middle and bottom rows*) of a nanosecond breakdown in air in time. Femtosecond-duration pulses short-circuit this process at multiphoton excitation, leading to both early- and late-time photon emission along the beam waist as the gas returns to the ground state. Three depictions of the recombination to the B state and successive emission to the A state are shown along the time axis to demonstrate the long-lasting emission useful for FLEET velocimetry. Nanosecond Rayleigh and femtosecond excitation images adapted with permission from Limbach (2015).

generate a pool of isolated electrons that, after hundreds of femtoseconds, gain kinetic energy via inverse Bremsstrahlung during the laser pulse, leading to cascade ionization of the gas when the free electron energy is higher than the ionization potential of the gas, producing optical breakdown. This bright spark at the laser focus emits a strong shockwave (Bak et al. 2015) and has a high temperature in excess of tens of thousands of degrees (Glumac et al. 2005), with an initial broadband (white) spectral profile that generates a hydrodynamic ejection to the surrounding flow (Brieschenk et al. 2013, Wang et al. 2020). **Figure 2** depicts some of these events in time, with a bright spark at nanosecond timescales (gated emission imaging), a shockwave at microsecond timescales (schlieren imaging), and the induced flow lasting milliseconds after the initial spark (schlieren imaging). Nanosecond breakdown is intrusive enough to be used as a source of flow control, as shown in both CFD (Kandala & Candled 2004) and experimental studies (Adelgren et al. 2005, Knight 2008, Osuka et al. 2014).

However, for femtosecond excitation, the comparatively impulsive temporal delivery of photons to the medium occurs within the mean free time for an electron to separate from its ionized source [300–800 fs in atmospheric air (Chin 2009)], preventing its participation in inverse Bremsstrahlung and the subsequent cascade ionization. These events that occur during

Inverse Bremsstrahlung: the increase in kinetic energy of an electron via the absorption of electromagnetic radiation

Mean free time: the average time between collisions of a particle (molecules, electrons, etc.)

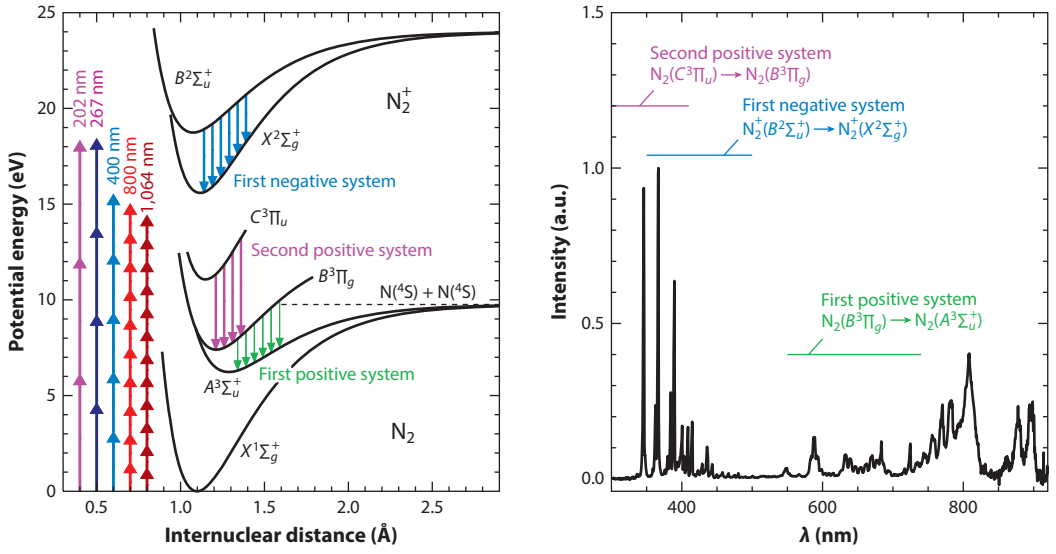

Figure 3

(*Left*) Representative energy level diagram with example FLEET photon energies for various wavelengths to demonstrate the required number of photons to reach an energy level by looking across the graph. (*Right*) A corresponding time-averaged spectrum, which has been corrected for the sensitivity of the spectrometer, highlighting the main emission components of the FLEET spectrum. Right panel adapted with permission from Burns et al. (2015).

femtosecond excitation predominantly result in the isolated multiphoton absorption events seen in **Figure 2**, the occurrence of which are typically masked in nanosecond-duration excitation by the greater electronic activity (Limbach 2015). Thus, femtosecond excitation allows for the repeatable deposition of energy along the beam waist as a fluorescence line (or even a filament) rather than a spark. Although a weak shock is generated along with some gas heating, neither is close to that experienced during a nanosecond breakdown. **Figure 2** depicts the early-time emission, initial shockwave, and late-time hydrodynamics of a nanosecond breakdown (emission and schlieren imaging), along with the similar Rayleigh scattering profiles of a FLEET line from Limbach (2015).

The emission spectrum of femtosecond filamentation is commonly referred to as clean (Talebpour et al. 2001, Chin 2009, Xu et al. 2009, Chin et al. 2012) in comparison to the nanosecond counterpart due to the lack of an optical breakdown and the limitation to species-specific multiphoton/tunnel ionization processes. This femtosecond excitation manifests itself in the spectral domain as isolated molecular and atomic emission peaks without a significant broadband component and in general is considered as follows (Michael et al. 2011, Miles et al. 2015), as shown in the energy level diagram and coupled time-average emission spectrum depicted in **Figure 3**. The UV portion of the spectrum is short lived (sub-microsecond) and is predominately due to the deexcitation of direct photo-ionization (~15.6 eV) and direct electronic excitation to elevated ro-vibronic levels (10–14 eV) in the form of first negative system emissions $[N_2^+(B^2\Sigma_u^+) \rightarrow N_2^+(X^2\Sigma_g^+)]$ and second positive system emissions $[N_2(C^3\Pi_u) \rightarrow N_2(B^3\Pi_g)]$, respectively. This short-lived emission [tens of nanoseconds in nitrogen at atmospheric pressure at 300 K (Edwards et al. 2015a)] is useful for fitting a gas temperature (Miles et al. 2015, Jiang et al. 2016) when calibrating for the FLEET-induced temperature increase, but it offers little use as a flow velocimetry instrument. However, photo-dissociation (~9.8 eV) of molecular nitrogen

along with other processes generates a pool of atomic nitrogen that promotes the rate-limiting recombination of atoms [$N(^4S) + N(^4S)$] to various ro-vibronic states in the *B* electronic level. This results in delayed emission from the first positive system [$N_2(B^3\Pi_g) \rightarrow N_2(A^3\Sigma_u^+)$] that lasts for tens of microseconds in the visible portion of the spectrum, offering the delay required to take useful time-gated images of the tagged molecules as they move in a flow.

Rate-limiting: the slowest step in a chemical reaction that governs the time to produce the final state

2.2. Excitation Frequency Considerations

The occurrence of multiphoton events without subsequent optical breakdown leads to significant freedom in the selection of laser frequencies when generating femtosecond filaments. While the pulse intensity to produce FLEET emissions does not necessarily reach femtosecond filamentation, most practical applications of FLEET do [calculated as a 388-μJ threshold at 800 nm for the setup from Gao et al. (2019)]. The high peak intensities afforded by femtosecond pulses permit the nonresonant multiphoton absorption required for FLEET generation with virtually arbitrary laser wavelengths. This kind of flexibility is not afforded by nanosecond pulses, which must be tuned to the vacuum UV for two-photon resonances. The variety of wavelengths utilized thus far and their benefits and drawbacks are discussed below.

2.2.1. Laser sources. The fundamental center wavelength of commercially available Ti:sapphire femtosecond regenerative amplifiers is near 800 nm (photon energy ~1.5 eV), which was the wavelength for the first demonstration of FLEET (Michael et al. 2011). Since then, different harmonics have been accessed with simple BBO (beta barium borate) crystal harmonic generation setups, including frequency-doubled lasers [400 nm/3.1 eV (Dogariu et al. 2019; Zhang et al. 2019b, 2020a)]; frequency-tripled lasers [267 nm/4.6 eV (Gao et al. 2019; Zhang et al. 2019b, 2020a)]; the selective two-photon absorptive resonance FLEET (STARFLEET), which operates at a frequency-quadrupled wavelength of ~202 nm/6.1 eV (Jiang et al. 2016, Reese et al. 2020) as shown in **Figure 4*a***; and the fundamental output of an Nd:YAG (neodymium-doped yttrium aluminum garnet) picosecond laser electronic excitation tagging (PLEET) system at 1,064 nm/1.2 eV (Jiang et al. 2017, Burns et al. 2018a). These photon energies are also featured in **Figure 3** for

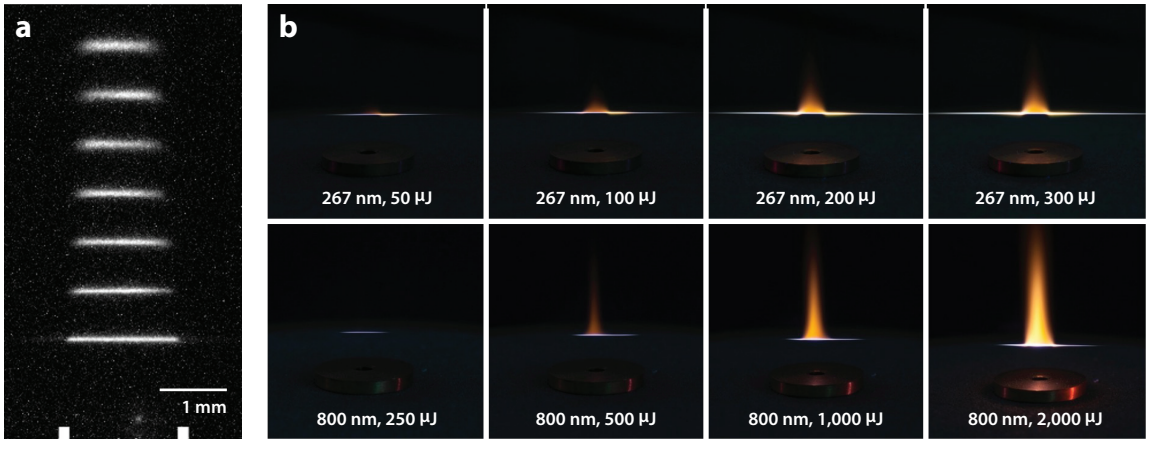

Figure 4

(*a*) Raw STARFLEET (selective two-photon absorptive resonance FLEET) emission lines in a nitrogen jet at 170 m/s. Panel *a* adapted with permission from Jiang et al. (2016). (*b*) Third harmonic FLEET compared to 800-nm FLEET images with a 20-s exposure in a nitrogen jet. Panel *b* adapted with permission from Gao et al. (2019).

direct comparison to energy levels of molecular nitrogen to illustrate the comparative number of photons required to excite certain states. With a higher frequency of input radiation, fewer photons and thus less pulse energy is required to elevate the molecule to the desired state. For example, only about three to four photons at 267 nm are required to ionize nitrogen, as opposed to ~10 photons at 800 nm. In addition, both Gao et al. (2019) and Zhang (2018) have shown the ability to produce longer, thinner tagging filaments with 267 nm at lower pulse energies, leading to an increase in measurement precision. Broadband time-averaged images from Gao et al. (2019) in **Figure 4*b*** illustrate the increased plasma emission over a longer line from 267 nm compared to 800 nm over a range of pulse energies. For the STARFLEET scheme, just two photons at ~202 nm resonantly excite the *C* state of N_2, leading to *C* to *B* emission, as well as long-lived *B* to *A* emission due to the rate-limiting atomic recombination of nitrogen. A disadvantage of FLEET is the high cost of the laser and detector hardware: Approximate costs in 2021 are $300,000 for a laser; $90,000 for a high-speed camera with a $70,000 high-speed intensifier or $70,000 for an intensified CCD (charge-coupled device) camera; $30,000 for optics and opto-mechanics; $35,000 for an oscilliscope and timing boxes; and, for STARFLEET, an additional $50,000 for a commercial fourth-harmonic generation system.

State-of-the-art, commercially available femtosecond amplifiers offer repetition rates in the range of 1–10 kHz, which remains inadequate for time-resolved measurements in many higher-speed flows. However, burst-mode laser sources have demonstrated short bursts of high-repetition-rate picosecond pulses for PLEET measurements at 100 kHz with a commercially available Nd:YAG system (Jiang et al. 2017, Hsu et al. 2020) and, recently, for FLEET measurements at 200 kHz with an Nd:glass system (Fisher et al. 2020b) on an experimental platform, with the possibility to expand to 1 MHz with the appropriate imaging hardware. High-speed intensifiers are now routinely coupled with high-speed detectors to image FLEET emission at these high repetition rates.

2.2.2. Energy deposition. While the fundamental laser output is the simplest option, it has been observed that the use of higher-energy photons can make the technique less intrusive (Jiang et al. 2016). While traditionally considered a nonintrusive technique in comparison to physical probes, FLEET is far from a disturbance-free method. The focused energy deposition leads to local gas heating, acoustic disturbances, and alterations to the local gas chemistry. Therefore, Jiang et al. (2016) consider FLEET as an often negligibly intrusive technique for many applications, rather than as broadly nonintrusive. A measure of the gas temperature has been obtained by fitting the rotational bands of the nitrogen second positive system emission from FLEET (Miles et al. 2015, Jiang et al. 2016) and from Rayleigh scattering measurements in delayed increments from the laser pulse (Limbach & Miles 2017), both of which have shown a temperature increase from laser heating. Several authors have estimated the effect of this local heat increase as an additional buoyant velocity, V_b, as a function of the ambient gas density ρ_a, the laser-heated flow density ρ_h, the acceleration of gravity g, and the delay time of a typical FLEET measurement $t = 10$ μs:

$$V_b = \frac{\rho_a - \rho_h}{\rho_h} gt. \quad 1.$$

For high-speed flow applications, V_b is a negligible percentage of the measured velocity and is often ignored even for near-infrared pulses in PLEET experiments (Jiang et al. 2017, Burns et al. 2018a, Hsu et al. 2020). However, Ryabtsev et al. (2014) demonstrated this local heating can lead to low-speed fluid motion due to the expanding gas from the filament by showing the similarities of the induced vortices from 40-fs, 800-nm, and 700-μJ pulses focused in air to those

produced from a heated wire. One possible solution to mitigate this heating is the selection of short-wavelength near-resonant excitation, as in STARFLEET (Jiang et al. 2016), which reduces the local heating from $\Delta T \sim 230$ K at 800 nm to just $\Delta T \sim 10$ K at 202 nm for similar signal levels [although the impact is intensity dependent (see Limbach & Miles 2017)], offering a more attractive option for lower-speed velocimeters or any application where local heating must be mitigated. In addition, making measurements near surfaces, such as in a boundary layer, is difficult given the high laser fluence and possible material damage and laser scatter. Once again, lowering the pump wavelength and decreasing the required pulse energy to produce similar-intensity FLEET lines can help the instrument approach or drop below the damage threshold of the object surface, allowing for measurements close to walls or surfaces (Dogariu et al. 2019, Zhang et al. 2019b).

Finally, the changes to the flow chemistry are important to consider to ensure measurements are performed in the desired test gas. While not meant for velocimetry, the purposeful addition of femtosecond filaments in premixed methane/oxygen/nitrogen flames with settings similar to those found in FLEET experiments (800 nm, 40 fs, ~2 mJ) has been shown to alter the natural flame structure, increase the flame speed, and increase the blow-off velocity for potential use as a flame-holding mechanism (Yu et al. 2010, 2012), suggesting care must be taken with FLEET velocimetry in combustion environments. Other work by Elias et al. (2018) in a Mach-3 flow showed significant flow perturbations, but with a 50-fs, 150-mJ source that is ~100 times that typically used for FLEET.

2.2.3. Acoustic disturbances. One observed drawback to the decrease in pump wavelength is the possible increase in acoustic disturbances in the flow (Zhang et al. 2020a). While the shock-wave produced by a focused femtosecond pulse is much weaker than a nanosecond breakdown (Limbach 2015) and decays to an acoustic wave (Mach 1) about 1 μs after the pulse, this disturbance can be measured with a microphone assembly (Zhang & Miles 2018b, Zhang et al. 2020a). While harmonic generation reduces the pulse energy achievable at lower wavelengths, Zhang et al. (2020a) has shown that the rate at which acoustic disturbances increase with pulse energy is higher for 400 nm than for 800 nm—specifically that 0.6 mJ pulses at 400 nm produced greater disturbances than 2 mJ pulses at 800 nm with a lens of $f = 250$ mm. These disturbances occur at the repetition rate of the laser system, which is typically 1 kHz, possibly adding an artificial frequency to the fluid environment that should be considered for acoustically sensitive flow studies. Edwards et al. (2015b) numerically and experimentally examined the effects of FLEET density perturbations on high-resolution turbulence measurements and showed no velocity errors for length scales longer than 100 μm. Therefore, while acoustic disturbances are weak, a balanced approach should be taken in the selection of excitation wavelengths to decrease the energy deposition while mitigating the acoustic disturbance.

2.3. Working Medium

The use of induced fluorescence for velocimetry depends on the longevity of the emitting medium. As explained previously, FLEET in nitrogen was originally found useful due to the rate-limiting recombination of dissociated nitrogen atoms to excited electronic states that emit in the visible spectrum over tens of microseconds. As of this review, only a decade has passed since the advent of this technique; therefore, it remains to be seen how many other species would exhibit similar behavior. The current media in which FLEET velocimetry techniques have been used include pure nitrogen, air, and cryogenic nitrogen (Burns et al. 2017); pure argon and argon–nitrogen mixtures (Zhang & Miles 2018a); pure R134a (1,1,1,2-tetrafluoroethane) gas and

R123a–air mixtures (Zhang et al. 2019a); water with phosphorescent supramolecules (Pouya et al. 2014); mixtures of nitrogen with helium, oxygen, and carbon dioxide (Calvert et al. 2016); room temperature methane–air and a mixture of methane–air combustion products (DeLuca et al. 2017, Zhang et al. 2018); and a premixed hydrogen/oxygen/nitrogen flame (Jiang et al. 2016). This list is sure to grow with time. In general, the FLEET signal is strongest in pure nitrogen environments, with the exception of the addition of helium or argon (Calvert et al. 2016, Grib et al. 2021), and the oxygen present in air causes increased quenching and a roughly tenfold decrease in signal compared to pure nitrogen (Michael et al. 2012).

2.4. Signal Characteristics

The intensity and lifetime of the FLEET signal, with regard to the initial thermodynamic state of the working medium, are not completely understood at this time. Early studies at subatmospheric pressures indicated a nonmonotonic behavior of both the signal intensity and lifetime (DeLuca et al. 2014); signal intensity decreased with decreasing pressure before increasing again at pressures below ∼250 Torr. The signal lifetime followed this same basic trend. These same studies indicated a nearly linear relationship between the laser energy and the observed signal intensity, despite the multiphoton nature of the excitation, which might be expected to have a nonlinear energy dependence. Later studies utilizing more sophisticated control of gas conditions confirmed these thermodynamic trends but showed the dependence to be principally based on flow density rather than pressure (Peters et al. 2020). At superatmospheric pressures, the signal intensity was found to scale linearly with gas density over temperatures between 145 and 275 K and pressures between 85 and 400 kPa (Burns et al. 2018b). Furthermore, the signal lifetime decreased with increasing density. It should be noted in all these data that absolute values of lifetime or trends in signal behavior do not exhibit a great degree of repeatability between measurement sets. The reasons for these discrepancies may lie in both the excitation method and the acquisition method. Differences in pulse energy, experimental setup, and chosen method of fitting the decay (single exponential, biexponential, or just reporting the $1/e$ value of the decay) may all contribute. Additionally, the delay at which the signal intensity is observed strongly influences the clarity of the observed trends, with shorter delays between laser pulse and image acquisition ($\lesssim$100 ns) yielding more pronounced trends with respect to the signal tendencies. This same trend was observed in FLEET concentration measurements as well (Halls et al. 2017). For a comparison of variations, readers are referred to Reese et al. (2020) for FLEET, PLEET, and STARFLEET signal trends and lifetimes in cryogenic flow environments.

3. FLEET SETUP AND IMAGING CONFIGURATIONS

Many variations of the basic FLEET setup exist, often tailored to specific applications. Broadly these measurement systems involve the generation and imaging of either lines or points. Each application typically requires a new set of analytical tools to analyze the data.

3.1. Signal Generation

The FLEET signal is generated along the beam waist of the optical path. Depending on the selection of focusing optics and the resolution of the detection system, the resulting tagged molecules may appear as a line or as a point in the flow.

3.1.1. Line generation. In the most common implementation of FLEET, a line of FLEET signal is excited by focusing the laser with medium- to long–focal length lenses (400–1,000 mm).

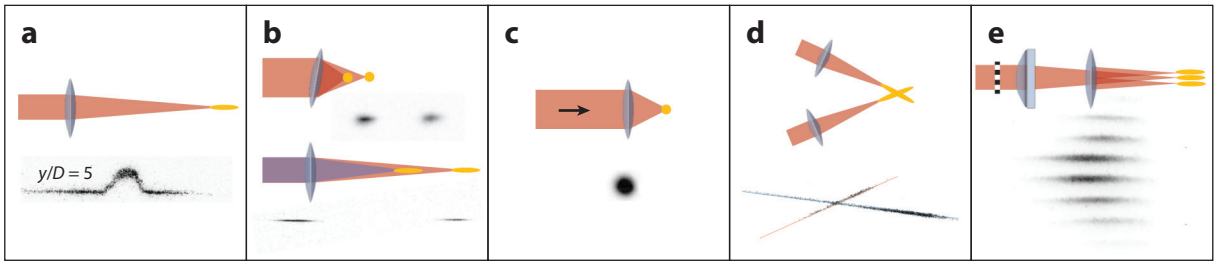

Figure 5

FLEET variations demonstrated thus far. (*a*) A standard FLEET line with a long–focal length lens. (*b*) Dual points or lines from lens astigmatism or chromatic aberration. Experimental images show (*top*) FLEET dots with a lens of $f = 63$ mm angled at 16° and (*bottom*) FLEET lines from an overlapped 400-nm and 800-nm source. (*c*) Point measurements with a short–focal length lens. (*d*) Multiple lines with different lens systems. (*e*) Multiline approaches taken by imaging light through spatial filters. Panels adapted with permission from (*a*) Michael et al. (2011), (*c*) Burns et al. (2015), (*d*) Zhang et al. (2019b), and (*e*) Zhang et al. (2020b).

The foundational experiments by Michael et al. (2011) utilized this strategy (with a lens of 500 mm focal length in **Figure 5*a***), as have many others. Typically, the line generated in this way is situated perpendicularly to the principal flow direction to allow the measurement of its velocity profile. In addition, sending multiple harmonics through the same singlet lens generates two spatially isolated lines by chromatic dispersion, as seen in the bottom of **Figure 5*b***. Alternative methods can be used to generate two or more FLEET lines for simultaneously imaging multiple components of velocity or multiple velocity profiles. Michael et al. (2011) demonstrated the generation of a cross (two lines) of FLEET signal. In these experiments, after the initial focus of the beam, the beam was reflected back through the focal region and refocused using a series of mirrors and a second lens (similar to those in **Figure 5*d***). Given sufficient space and resources, entire grids can be generated in this manner. An alternative strategy was presented by Zhang et al. (2020a) and Marshall et al. (2021) for use in generating parallel FLEET lines. As shown in **Figure 5*e***, this method utilizes periodic masks placed within the femtosecond laser beam. When the masked beam is focused through a series of lenses (cylindrical and spherical), a series of parallel FLEET lines is generated, the spacing of which is dependent on the slit width and the spacing used in the masking procedure. This method could be used to simultaneously observe multiple velocity profiles.

3.1.2. Point generation. The generation of points of FLEET signal has seen a number of applications. While the measurement of velocity derived from FLEET points is innately zero dimensional, imaging of points is advantageous over line imaging in that it can provide multiple components of velocity simultaneously. The generation of points of FLEET signal is typically achieved by using short–focal length lenses (<250 mm) (Burns et al. 2015). **Figure 5*b,c*** depicts point schemes, with the point scheme in **Figure 5*b*** utilizing lens astigmatism to generate two points using a single lens. Very tight focusing with such lenses shortens the line but also increases the diameter of the line, making the signal generated in this way a good approximation for a point (reported as a 1-mm diameter by a 2-mm-long point). Point imaging has been used for two- and three-component velocity measurements (Danehy et al. 2014, Burns et al. 2015) and for 2D measurements when combined with a scanning system (Burns & Danehy 2017).

3.2. Imaging Strategies

There are several common imaging strategies utilized to image both FLEET lines and points. These strategies can be broadly classified by imaging configuration and data acquisition strategy.

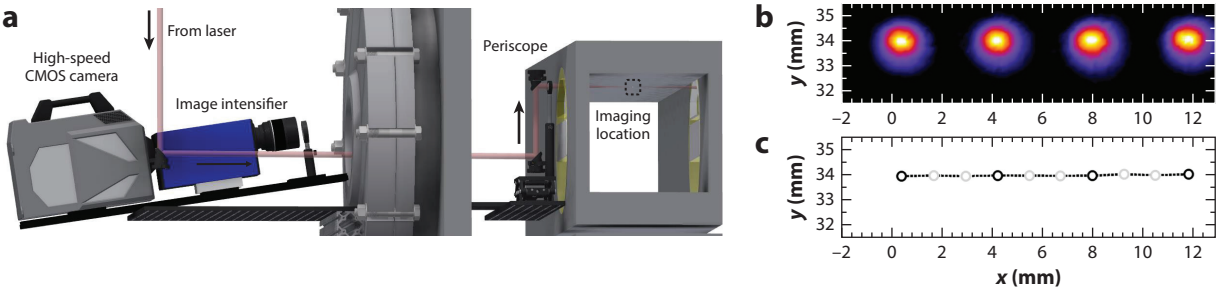

Figure 6

(*a*) A boresight optical FLEET setup in a wind tunnel. (*b*) Overlaid experimental FLEET images recorded at different time delays. (*c*) The measured trajectory from panel *b*. Figure adapted with permission from Burns & Danehy (2017). Abbreviation: CMOS, complementary metal-oxide-semiconductor.

The most common imaging configuration is orthogonal viewing. The foundational FLEET experiments (Michael et al. 2011) utilized this strategy, where a focused femtosecond beam was positioned over an axisymmetric jet and imaged orthogonally by a gated, intensified CCD camera. Another common imaging configuration is the boresight method (Zhang et al. 2016), in which the FLEET signal is imaged along or nearly along (known as quasi-boresight) the direction of beam propagation. Burns et al. (2015) and Burns & Danehy (2017) utilized this strategy extensively due to the physical constraints of the wind tunnel in which the work was done, but also in order to measure two orthogonal components of velocity (see **Figure 6**). Because this method spatially integrates the signal along the beam path, it is best reserved for the imaging of a point FLEET signal. Another imaging configuration employed by Danehy et al. (2014) was a split-view system. This system utilized two imaging periscopes coupled to the same lens to image a FLEET spot from two orthogonal directions (**Figure 7**). This system enabled three-component velocity and acceleration measurements.

In addition to the physical configuration of the camera/lens systems with respect to the FLEET signal, the data acquisition strategy is another important element of the FLEET signal

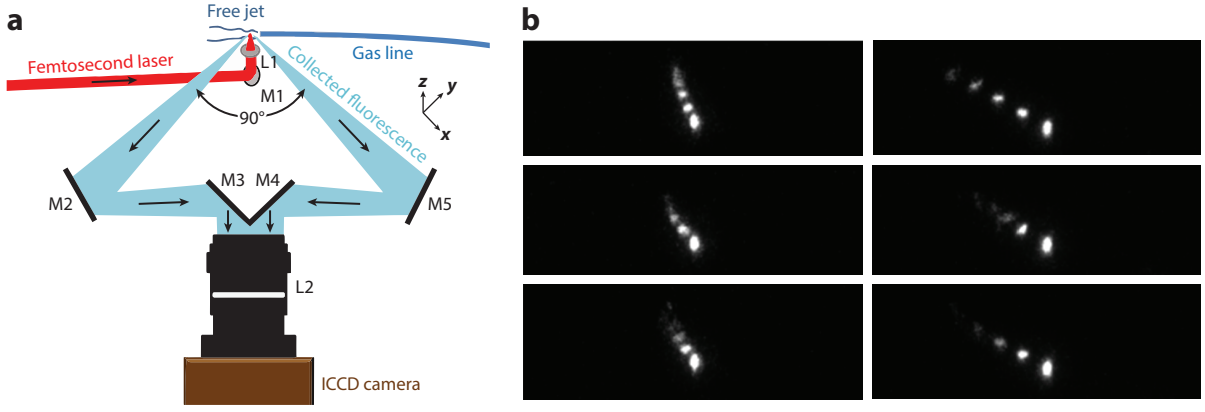

Figure 7

(*a*) Split-view of a FLEET point experimental setup where M1–M5 are mirrors, L1 is a spherical lens with 50-mm focal length, and L2 is an *f*/1.5 camera lens with 50-mm focal length. (*b*) Each row shows the split-view pair of images of the same FLEET point at five successive exposure times. Figure adapted with permission from Danehy et al. (2014). Abbreviation: ICCD, intensified charge-coupled device.

imaging. One strategy employed by Michael et al. (2011) is the single-exposure method. The single-exposure method evaluates signal displacements by comparing a FLEET line independently imaged shortly after the laser pulse with displaced FLEET signals acquired in separate data runs or at different times. This method is versatile in that it allows for the widest range of equipment to be utilized; the camera system only needs to be able to trigger and gate at an integer divisor of the laser frequency in order to acquire signal. However, because the signals in the initial and displaced frames are acquired at different times, instantaneous irregularities in the FLEET signal profile and longer-term changes in beam position (caused by vibrations, for example) and profile are not accounted for in the data acquisition, leading to increased uncertainty. Such errors can be reduced by acquiring multiple exposures from the same laser pulse, providing a signal and reference for each pulse. One way to do this is called multigate imaging, in which multiple intensifier gates are acquired on a single camera exposure. This method allows the rate at which the signal is sampled to be partially decoupled from the camera frame rate; for example, by allowing the camera to acquire images at 1,000 Hz but gating the image intensifier at 100 kHz, many frames may be captured within the same exposure. This method was used by Reese et al. (2021) in measuring freestream and wake velocity profiles (introduced and detailed in Section 4.2.2) and in the images shown in **Figure 7*b***. Unlike the single-exposure method, this strategy acquires both the initial and displaced FLEET signals simultaneously, eliminating errors associated with using separate mean data sets. Since the multigate imaging method relies on advection of the FLEET signal to spatially separate subsequent intensifier gates on the images, it is well suited to flows that possess high velocities and minimal flow gradients that could result in overlap of signal from subsequent gates. Burst imaging is another data acquisition method appropriate for imaging a FLEET signal. As used by Burns et al. (2015), Burns & Danehy (2017), and others, burst imaging utilizes a high-speed camera and intensifier system to acquire a series of images after each femtosecond laser pulse, imaging, for example, a burst of 10 images at 200 kHz. This method acquires the initial signal position and those at numerous displacement frames. Since each image only contains data from one intensifier gate, there is no possibility of the signal overlapping, as is the case with the multigate method. However, the high frame rates necessitated by this method typically reduce the usable area on the image sensor, limiting the allowable displacements. This method is well suited to regions of lower velocity, or regions of high unsteadiness or recirculation in which the likelihood of signal overlap with other methods is high. Finally, a high-speed PLEET system utilizes a combination of these methods by operating the laser at 25 kHz while acquiring images at 100 kHz to collect a long history of the flow spots in each frame (Burns et al. 2018a).

3.3. Fitting Procedure

Unlike more established techniques such as PIV, there is not currently a standardized method for processing FLEET images to compute velocity. Instead, group- or individual-specific codes are typically used, which are customized to the many acquisition methods and experimental setups. Most FLEET analyses utilize some form of fitting procedure to discern signal centroid locations within acquired images. For typical 1D line velocity measurements, the streamwise intensity profiles are usually fit with a Gaussian line-shape, although Voigt and Lorentzian profiles may serve as a better fit at early time delays (Dogariu et al. 2019). Subpixel resolution is commonly achieved with an accuracy of 0.1 pixels for earlier MTV work by Gendrich & Koochesfahani (1996). For FLEET point measurements, this same general approach can be used, wherein an axisymmetric Gaussian surface is fit to the 2D FLEET image. However, due to the nonspherically symmetric shape of FLEET spots, often some variation of this method is employed in practice, such as the intensity-weighted centroid position (Danehy et al. 2014) or the SRGE (shifted, rotated, generic ellipsoid) fit method detailed by Burns et al. (2018b).

Another common strategy in the evaluation of FLEET signal positions and displacements is the use of cross-correlation. Cross-correlation provides a direct measurement of FLEET signal displacements rather than absolute positions. The primary advantage of cross-correlation is the acceptance of a wider array of signal shapes, since the signal does not need to fit a specific template in order for cross-correlation to work. Both FLEET point (Peters et al. 2016, Burns & Danehy 2017) and line (Hill et al. 2021) measurements have used this method, and it is common in other MTV line evaluation schemes.

3.4. Practical Details

There are several practical considerations to be made in constructing and working with a FLEET measurement system and analyzing FLEET data. These include, among others, considerations about signal formation, intensity, and lifetime; issues related to the propagation of femtosecond-duration pulses through glass; and considerations of spatial resolution.

3.4.1. Signal intensity and lifetime. The quality and character of the FLEET signal generated by a given system is a function of numerous parameters, including the laser pulse energy, beam quality, pulse duration, and the focusing lens used in generating the signal. Of practical concern in setting up a FLEET system is the selection of the focusing lens to be used for a given application. Short–focal length lenses tend to generate shorter lines of FLEET signal with larger diameters, while longer–focal length lenses generate lines that get progressively longer and thinner as the focal length is increased. The signal generated by particularly short lenses ($\lesssim$100 mm) is often indistinguishable from a sphere. The freestream and airfoil measurements by Burns et al. (2017, 2018b) utilized this phenomenon to make two-component point measurements in the NASA Langley 0.3-m Transonic Cryogenic Tunnel. Related to this focal length dependence is the apparent increase in signal intensity and lifetime with increasing local laser intensity. That is, as the intensity of the beam is increased through focusing or increasing energy, the lifetime and intensity of the signal tend to increase. Reese et al. (2021) noted this in velocity profile measurements, in which the FLEET lines seemed to shorten in time because the signal intensity was lower and becomes unobservable near the start and end of the line, and this same signal exhibited shorter lifetimes. Thus, selection of lens focal length and pulse energy must be made in consideration of the long-term behavior of the signal, rather than just the initial character of the FLEET line.

Another phenomenon related to the signal intensity and lifetime was noted by Burns & Danehy (2017), in which the FLEET signal lifetime decreased by over an order of magnitude in regions of elevated turbulence or separated flow; these data were collected in the near-field wake and near-surface flows of a transonic airfoil flow field. It was unclear if this effect resulted from the local turbulence interfering with the formation of the FLEET signal, or if high strain rates and the increased turbulent diffusion broke up the pool of dissociated nitrogen atoms, reducing the observed lifetime of the FLEET signal in these regions. Burns & Danehy (2017) estimated the timescales associated with the local turbulence to range from about 30 μs for the outer flow down to 200–300 ns for the mixing timescales, all of which were longer than the observed signal lifetimes and initial signal delay but were similar in length to the duration over which the fluid trajectories were measured. This uncontrolled signal decrease prevented the use of FLEET for measuring the gas density with either the signal intensity or lifetime throughout the airfoil flow field.

3.4.2. Lens and window requirements. Free-space propagation of the femtosecond-duration pulses used in FLEET measurements often poses little challenge to the setup and execution of experiments. However, when working in and around wind tunnel facilities, special consideration

is needed when transmitting these pulses through windows and lenses. One major consideration when selecting a lens or window material is the group velocity dispersion (GVD). Due to the broadband nature of typical femtosecond pulses, optical materials such as BK-7 can cause a dispersion effect that results in chirping. While adjustments can be made to counteract this effect within the compressor of most commercially available lasers, avoiding the issue altogether is better when possible. A shorter temporal pulse increases the peak power and more efficiently generates FLEET emission, but it contains a broader spectrum, leading to increased concern over the GVD of the optics. Therefore, a trade-off between peak power and pulse chirp must be considered and will be application dependent. Glasses such as fused quartz, fused silica, calcium fluoride, and magnesium fluoride have superior GVD properties, wider optical transmission bands, and higher damage thresholds, which make them better choices when working with femtosecond-duration lasers.

GVD: group velocity dispersion, which is the variation in propagation speeds through a medium as a function of wavelength

Chirping: lengthening of the pulse in both time and physical space as the different colors separate, often because of dispersion that varies with wavelength

Astigmatic propagation: the propagation of a laser beam through a lens at an angle, or off-axis transmission

Also associated with the transmission of femtosecond pulses through windows is the effect known as white light generation. This phenomenon is the volumetric broadband emission caused as a high-intensity laser transmits through glass. In practice, white light generation only occurs above a certain threshold of laser intensity, below which light transmission is largely unabated by the glass beyond simple reflective losses. Above this threshold, the transmission through the glass drops off precipitously, and extended time spent in this state can cause permanent volumetric damage to the window or complete breakage. A window surface free of scratches and pitting tends to increase the intensity threshold at which this phenomenon occurs. Practically, white light generation can limit the overall laser energy used in a given experiment and must be considered in the experimental planning for both the FLEET measurements and the safety of facilities and personnel. Another consideration when working with femtosecond laser systems is the overall tolerance to transmission energy losses. If the application relies on very low pulse energy (<100 μJ) or shorter UV wavelengths, where pulse energy is minimal due to losses associated with harmonic generation, such as in STARFLEET, it may be necessary to select window materials such as magnesium fluoride or calcium fluoride and appropriate high-reflectivity mirrors to prevent excessive energy loss before the focusing optics (Zhang & Miles 2018a; Reese et al. 2019b, 2020; Zhang et al. 2019b, 2020a).

The propagation of femtosecond-duration pulses through lenses also poses more difficulty than traditional nanosecond-laser pulses in that astigmatic propagation through lenses can lead to significant losses in FLEET signal intensity and overall character. For small misalignments (<6°), the principal effect is a loss in the resulting FLEET signal intensity and a slight increase in the length of the FLEET signal. For larger misalignment angles, a phenomenon in which two separate FLEET spots form has been observed (shown previously in **Figure 5*b***), one at the horizontal focus and one at the vertical focus, with greater angles leading to a greater separation between the two spots. The signal intensity decreases by orders of magnitude when this separation into multiple spots occurs. In practice, care must be taken when assembling FLEET optical systems such that off-axis propagation is avoided, and if the system is enclosed or not accessible during experiments, remote adjustments to correct for these errors are advised.

3.4.3. Spatial resolution and velocity determination. The method used in evaluating the velocity limits the spatial resolution of FLEET measurements. Particularly with the use of multigate imaging (Reese et al. 2021) and burst imaging (Burns et al. 2017), there are commonly more than two acquired emission locations available for evaluating the velocity with FLEET data. While these data are advantageous in that they can enable the determination of fluid trajectory, including velocity and acceleration, an unintended consequence of fitting methods such as linear regression, polynomial fitting, or skipping frames is the loss of spatial resolution. Using these

methods often yields improved measurement precision (Burns et al. 2015), but if the model used in fitting the trajectory is inappropriate, the spatial information contained in the path can be lost, improving the measurement precision at the cost of the spatial resolution. Careful attention to the statistical weighting of polynomial coefficients and general observation of the signal trends can prevent this loss of information and improve the measured velocities. In addition, FLEET velocimetry between two successive emission locations is the average velocity over the spatial increment, effectively filtering the contributions of subdisplacement length scales. Therefore, for measurements in turbulent flows, the turbulence spectrum should be considered when selecting FLEET displacements and the magnification of the imaging system.

4. APPLICATIONS

Since its inception, FLEET has been used in a variety of fluid flows from simple benchtop testing to large-scale, high-speed ground test facilities. This section highlights testing in these small-scale developmental studies, while focusing on a few high-impact results from large-scale ground test facilities. For diagnostic platforms that utilize FLEET for purposes other than velocimetry or that couple FLEET with other instruments to add velocimetry to existing systems, please see the sidebar titled Multiparameter Measurements and **Figure 8**.

4.1. Benchtop Testing

The majority of the early work on FLEET was from the founding group at Princeton, performing mostly small-scale yet highly informative developmental work. There are several studies regarding some fundamental properties and limitations of FLEET, such as studies of the limitations of turbulence measurements (Edwards et al. 2015b), methods to obtain boundary layer profiles (Calvert et al. 2013), two-component measurements with vorticity (Calvert et al. 2014), studies concerning the precision of a FLEET instrument with different detector hardware options (Peters et al. 2015), high-speed pipe flow comparisons to hotwire measurements (Zhang & Miles 2017), and studies of the effectiveness of FLEET in measuring shear flows (Zhang et al. 2016).

Unique applications of FLEET to date include velocity measurements in water (Pouya et al. 2014), profiles of the exhaust of pulsed detonation engines (DeLuca et al. 2017), measurements in a premixed methane flame (Zhang et al. 2018), external and internal velocity measurements of a sweeping jet actuator (Peters et al. 2016), FLEET and PLEET measurements with a hollow-core fiber system (Hsu et al. 2018a), velocity maps of a nanosecond breakdown shockwave and hydrodynamics (Nishihara et al. 2020), measurements in a bladeless turbine (Fisher et al. 2020a), and measurements as a laser guide in the FAILED (filamentary anemometry using femtosecond laser–extended electric discharge) technique (Li et al. 2018).

4.2. Subsonic/Transonic

Traditionally the domain of PIV techniques, FLEET has now also found a home in subsonic/transonic flows as a seed-free alternative.

4.2.1. FLEET on a transonic airfoil. FLEET was used by Burns & Danehy (2017) in the NASA Langley 0.3-m Transonic Cryogenic Wind Tunnel, a pure nitrogen environment, to characterize the flow field around a semispan transonic airfoil. The experiments utilized a commercial femtosecond laser system (1 kHz, 800 nm, 1 mJ/pulse, 70 fs). FLEET measurements were conducted in the quasi-boresight imaging configuration, and the measurement location was translated to different positions around the airfoil using a series of adjustable periscopes installed within the

MULTIPARAMETER MEASUREMENTS

While only discussed as a velocimetry technique thus far, when simultaneously spectrally or temporally resolved, FLEET emissions can also be utilized for measurements of temperature, species concentration, and even pressure with a few underlying assumptions. Edwards et al. (2015a) demonstrated spatially resolved measurements of temperature by imaging the FLEET emission along a line in a heated jet to a spectrometer and fit the second positive and first negative systems for temperatures up to 650 K with Specair (Laux 2002). The FLEET emission is weak; therefore, a precision of 10% required the accumulation of 1,000 laser shots. However, care must be taken to properly account for the heat added to the gas from the FLEET process itself. Halls et al. (2017) measured the nitrogen/oxygen mixture ratio in jet flows from the FLEET signal intensity with a previously determined calibration of the intensity of the FLEET signal with different nitrogen/oxygen mixtures for specific gate and delay times. Burns et al. (2016) measured flow velocity and density from a combined Rayleigh/FLEET instrument in a cryogenic wind tunnel and inferred the temperature and pressure from the FLEET intensity with an iterative approach by assuming a constant total enthalpy and a constant species concentration. This method required calibration of the density instrument with a secondary density measurement provided by the facility data acquisition system. Finally, as a simple implementation technique, FLEET can easily be combined with other diagnostics to add velocimetry to a laser-based measurement platform for other thermochemical quantities of interest.

Since FLEET is a simple optical technique, perhaps the most promising future multiparameter measurements with FLEET are also multitechnique, where FLEET adds velocimetry to an existing optical diagnostic platform. One such example is FLEET with hybrid femtosecond/picosecond coherent anti-Stokes Raman scattering (CARS) for velocity and rotational/vibrational thermometry (Dogariu et al. 2021) and even pressure (Dedic et al. 2019). **Figure 8** shows recent but unpublished work by the authors of average rotational temperature and pressure measurements from CARS (Kearney et al. 2020), as well as velocity from FLEET in an underexpanded sonic jet along a measurement line 15 mm downstream of the jet exit, demonstrating the potential of adding FLEET velocimetry to scalar measurements in a supersonic flow.

plenum of the wind tunnel. The laser was not translated closer than 1.5 mm from the surface to prevent damage to the model. Two-component velocity profiles were evaluated at 12 different positions (10 along the chord of the airfoil and 2 in the wake). Measurements were made at a freestream Mach number of 0.85 (~270 m/s) with the airfoil at a 7° angle of attack. Unlike previous studies using the quasi-boresight imaging configuration (Burns et al. 2015), these FLEET data were analyzed using an adaptive cross-correlation scheme instead of a surface-fitting method

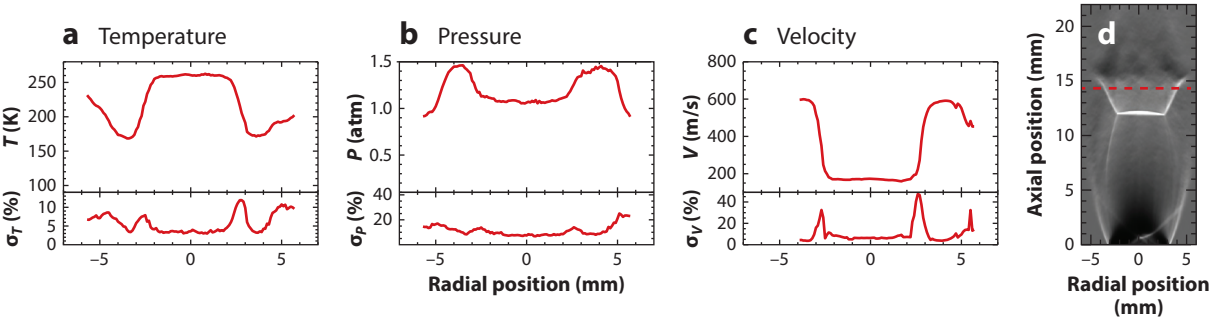

Figure 8

Average and standard deviation radial profiles of (*a*) rotational temperature, (*b*) pressure, and (*c*) velocity at an axial location 15 mm downstream of a sonic jet exit, as marked on a representative (*d*) average schlieren photograph. The average measurements are over 120 laser shots.

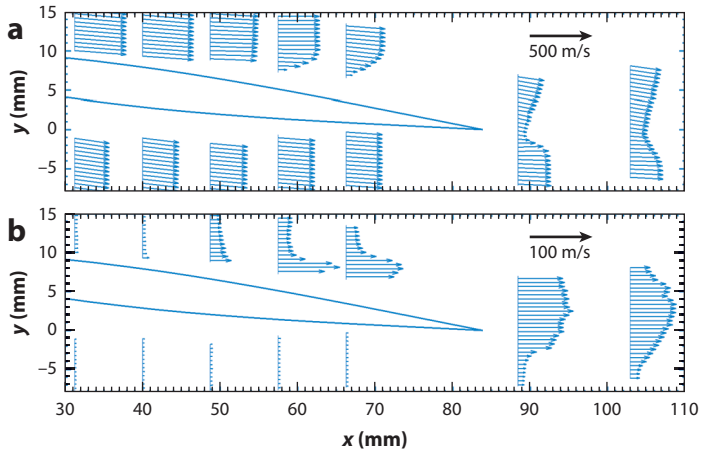

Figure 9

(*a*) Mean velocity vectors and (*b*) fluctuating velocity $[(\langle u'_x \rangle^2 + \langle u'_y \rangle^2)^{1/2}]$ from FLEET measurements on a transonic airfoil. Figure adapted with permission from Burns & Danehy (2017).

to accommodate widely varying spot shapes. A four-point trajectory was measured instead of a single velocity, and different velocity evaluation methods were employed in different regions of the flow where appropriate.

Figure 9 depicts the measured velocity profiles around the airfoil along with the fluctuating velocity. The measured velocities behaved predictably; fully attached flow was observed on the lower (compressive) surface of the airfoil, while regions of both supersonic and separated flow were found on the upper surface. The errors were found to lie between 1 and 1.5% of the measured velocity, while the measurement precision was between 1 and 4.6 m/s depending on the method of evaluation used in the FLEET trajectory measurements. The instrument exhibited worse precision in regions of separated flow, found on the upper surface of the airfoil and in the nearfield wake, due to the shorter FLEET signal lifetime in these regions.

4.2.2. FLEET in a large-scale transonic cryogenic tunnel. The FLEET technique has been implemented (Reese et al. 2019a, 2021) in the NASA Langley Research Center's National Transonic Facility (NTF), which is the world's highest Reynolds number transonic wind tunnel (Wahls 2001). The NTF operates on air, nitrogen, or a mixture of the two. It uses cryogenic nitrogen addition and high pressure to produce high–unit Reynolds number transonic flow in its 2.5-m square cross section. Temperatures as low as 116 K and total pressures as high as 860 kPa can produce unit Reynolds numbers exceeding 400 million/m, which is sufficient to test the largest aircraft in service today (Wahls 2001).

Since the NTF can operate on pure N_2 and the gas density is very high during cryogenic operation (up to 22 times atmospheric density), the FLEET method, which has a signal intensity proportional to gas density for densities in this range (Burns et al. 2018b), is an attractive measurement technique for use in the NTF. However, there are several aspects of implementing FLEET in the NTF that are challenging. First, the test section is enclosed in a windowless pressure shell. Second, the high gas densities combined with turbulent fluid currents in the plenum between the test section and the outer shell would affect the alignment of the FLEET laser beam. A dedicated optical system has been implemented to circumvent these two problems that passes the laser light through windows mounted at both ends of a heated, insulated, and evacuated tube

Reynolds number: the ratio of inertial forces to viscous forces within a fluid, used to scale fluid mechanical experiments

Unit Reynolds number: the Reynolds number per characteristic length (Re/L)

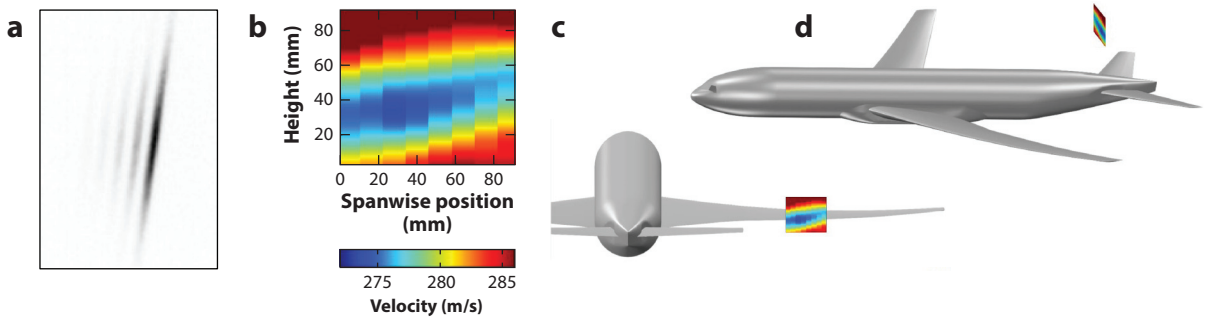

Figure 10

Averaged, raw FLEET data obtained at one spanwise position (*a*) with the laser passing from top right to bottom left and the flow moving right to left. The spacing between the lines is about 5 mm. The resulting velocity map (*b*) shows the velocity deficit in the wake of the wing. The data plane has been placed on a rendering of the model in panels *c* and *d*. Figure adapted with permission from Reese et al. (2021).

that penetrates the outer pressure shell. Since there is not a straight path from the tunnel exterior to the test section, remote-controlled mirrors are required to direct the light to the tunnel. A third challenge involves tightly focusing the light about 1.3 m to the tunnel center line through existing window ports 152 mm in diameter located on the top of the test section. A combination of lenses configured as a Galilean telescope is used to first expand the beam and then focus it into the tunnel.

To detect the FLEET signal, researchers have mounted a lens/intensifier/camera system behind a side wall window 203 mm in diameter in a canister that is held close to atmospheric pressure and room temperature. This system, including the camera focus, can be remotely operated from the control room. Since the laser window on the top of the test section does not align with the side wall window where the camera is located, the resulting FLEET signal appears as diagonal lines, as shown in **Figure 10*a***. These data, obtained in air, were acquired by operating both the camera and laser at 1 kHz while the intensifier triggered the gate multiple times for each laser pulse.

Freestream measurements in air and N_2 showed good agreement with the operating conditions from the NTF instrumentation (typically within 1%). In air, only averaged measurements were obtained. In N_2, instantaneous measurements showed a precision of 1% (Reese et al. 2021). Planar measurements were desired in a test involving the NASA full-span Common Research Model, which is an aircraft model developed for fundamental investigations of transonic flight (Vassberg et al. 2008). This measurement was performed to provide quantitative velocity data in the wake of the wing for comparison with CFD while also providing an opportunity to mature the measurement technique. To generate a 2D map of the flow, researchers attached remotely controlled motors to the last turning mirror in the optical path, allowing the laser to be scanned toward and away from the camera; the camera was remotely refocused at each position. The model was also rolled ±3 degrees to extend the measurement plane vertically. **Figure 10*b*** shows the resulting velocity map, which quantifies a ∼5% (∼12 m/s) velocity deficit. **Figure 10*c,d*** shows this measurement plane superimposed on a rendering of the model. The paper shows a favorable comparison between this velocity map and a CFD solution (Reese et al. 2021).

4.3. Hypersonic

In contrast to subsonic/transonic flows, seed-based velocimetry methods are uncommon in hypersonic flows due to particle lag concerns. Molecular tagging velocimetry techniques such as FLEET are well suited for hypersonic flows.

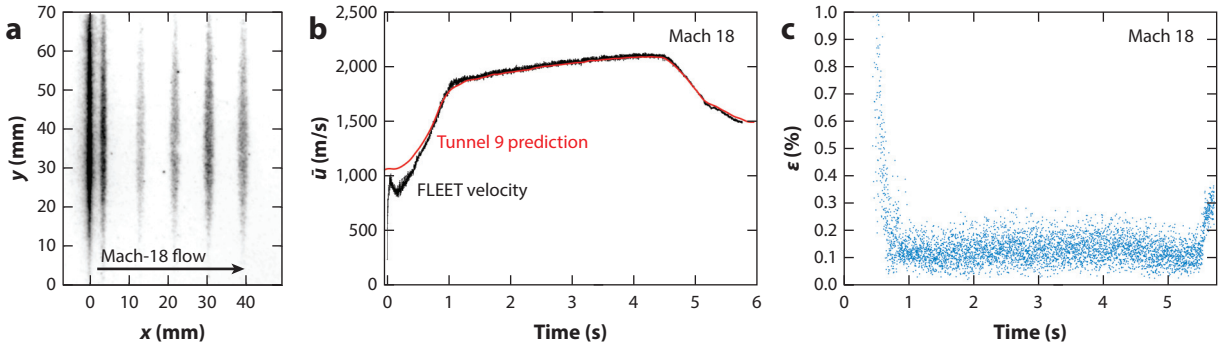

Figure 11

(*a*) Raw FLEET images, (*b*) velocity results, and (*c*) uncertainties for freestream measurements in Arnold Engineering Development Complex Hypervelocity Wind Tunnel 9 at Mach 18. Figure adapted with permission from Dogariu et al. (2021).

4.3.1. Hypersonic freestream flows. Dogariu et al. (2019) demonstrated the first use of FLEET in the Arnold Engineering Development Complex Hypervelocity Wind Tunnel 9 with a portable laser system (1 kHz, 800 nm, 7 mJ/pulse, and 100 fs, with an option for 400 nm) at Mach 10 (~1,476 m/s) and Mach 14 (~1,920 m/s) in pure nitrogen flows. Recently, the same group has expanded the technique to Mach 18 flows with a coupled hybrid CARS instrument (Dogariu et al. 2021) to measure nonequilibrium rotational and vibrational temperatures. **Figure 11** depicts the freestream measurements at Mach 18. Excellent agreement is achieved with the tunnel predictions, with random uncertainties below 0.3% during the few seconds of steady flow conditions. Systematic studies on the effect of gate delay time with measurement error encouraged the use of delays from 10 to 20 μs to mitigate errors from either a short line displacement or the decreased signal-to-noise ratio (SNR) for later delays.

A few recent FLEET (Fisher et al. 2021) and PLEET (Hsu et al. 2020) studies in Mach-6 flows also demonstrated effective freestream measurements. Fisher et al. (2021) implemented FLEET in the Boeing/Air Force Office of Scientific Research Mach 6 Quiet Tunnel (BAM6QT) at Purdue University. As a quiet tunnel, the nozzle needs to be highly polished, which precludes the use of any seed-based technique, necessitating an MTV technique for off-body velocimetry. The authors utilized the fundamental output of a 1-kHz femtosecond amplifier at 800 nm with a pulse energy of 1.4 mJ and a duration of 160 fs, both measured inside the test section after the facility windows, to write an ~10-mm FLEET line that was recorded on a coupled high-speed intensifier and detector with 10 sequential 500-ns gates at 250 kHz with a 93% gain. To maximize the signal, researchers used pure N_2 as a test gas over the several-second test time. A measurement accuracy of 1.5% with a precision of 0.33% was demonstrated in the Mach-6 freestream flow (static temperature and pressure of 51 K and 150 Pa, respectively). As a freestream measurement with nominally single-component flow, the spatial resolution of the FLEET instrument was degraded to improve the SNR by binning the entire FLEET line emission to a single point. The 1.5% accuracy was determined from the facility probe measurements, which themselves have 1.75% uncertainty. The use of additional FLEET exposures to measure the flow velocity improved the precision, but only for exposures with sufficiently high SNRs. Uncertainty inherent in the measurement from the spatial calibration and the subpixel fitting procedure prevented the instrument from measuring the expected $<0.1\%$ velocity fluctuations in the facility.

SNR: signal-to-noise ratio

4.3.2. Hypersonic boundary layer and wake measurements. Each hypersonic freestream application discussed in Section 4.3.1 also evaluated FLEET's ability to provide detailed boundary

RANS: Reynolds-averaged Navier–Stokes

layer or wake measurements. The boundary layer of a hollow-cylinder/flare test article was measured by Dogariu et al. (2019) with both a normal and tangential configuration to the test article. The average boundary layer profiles were compared to previous PIV measurements and RANS (Reynolds-averaged Navier–Stokes) CFD simulation results, where both the PIV and FLEET Mach-10 cases matched turbulence intensities in the boundary layer within 25%. Fisher et al. (2021) placed a turning mirror and focusing optic on a translation stage to move the physical position of the FLEET line over 10 runs to map out the boundary layer profile of a 5° half-angle cone-cylinder/flare test article. The results demonstrated good agreement with a CFD solution obtained utilizing the axisymmetric STABL2D (stability and transition analysis for hypersonic boundary layers) code developed at the University of Minnesota. Researchers at Sandia National Laboratories used a 1-kHz, 100-fs amplifier system and BBO crystals to generate the second and third harmonics from an 800-nm source to generate FLEET lines in the hypersonic wind tunnel to measure wake flows of a 7° half-angle cone model (Zhang et al. 2019b). In this work, FLEET lines with 276 nm were three times longer and 25% thinner than with 800 nm (after 1 μs); the thinner line potentially improved measurement precision, but utilizing the third harmonic required the use of MgF_2 windows to transmit the UV light, and after optical losses only 42% of the generated 276 nm was measured in the test section, consistent with the observations of Reese et al. (2019a, 2020).

Another recent measurement demonstrated FLEET's potential for studying the dynamics of laminar and turbulent boundary layers. Hill et al. (2021) extracted 1D velocity profiles in boundary layers from pure nitrogen flows around an ogive-cylinder model in the Air Force Research Laboratory's Mach-6 Ludwieg tube. In this work, the researchers investigated the effects of model tip bluntness at unit Reynolds numbers ranging from 3.4×10^6/m to 3.9×10^6/m. By directing the laser to create the FLEET line into a 3.8-mm-diameter pressure sensor port on the model, the authors were able to avoid the significant surface plasma that prevents the camera's ability to resolve velocity measurements, yielding boundary layer measurements closer to the model surface than is possible in other FLEET studies (Dogariu et al. 2019). A schematic of the ogive cylinder showing details for dumping the FLEET beam inside the model is shown in **Figure 12*a***, while the write

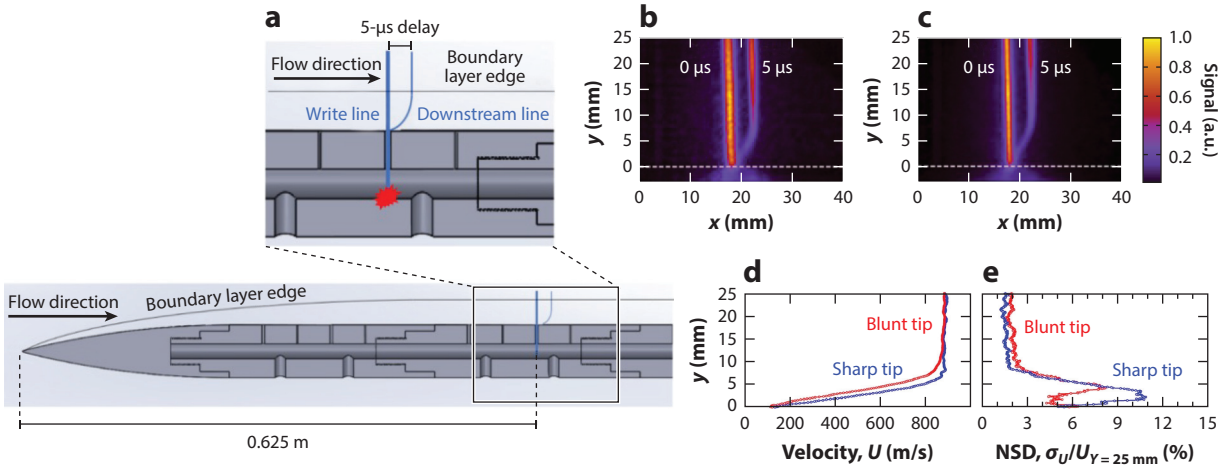

Figure 12

(*a*) Schematic of the ogive-cylinder model used in the hypersonic boundary layer FLEET experiment (Hill et al. 2021). (*Inset*) Details for dumping the FLEET beam inside the model. (*b*,*c*) Superposition of the write and read FLEET lines used to calculate flow velocity for the (*b*) sharp-tip and (*c*) blunt-tip models. (*d*) Mean velocity profiles and (*e*) normalized standard deviation (NSD) profiles measured for the sharp-tip and blunt-tip configurations. Figure adapted with permission from Hill et al. (2021).

and read lines (acquired separately, but superimposed in the figure) used to calculate flow velocity for the sharp-tip and blunt-tip models are shown in **Figure 12*b*** and **12*c***, respectively. By cross-correlating the write line with the read line (captured at a delay of 5 μs), researchers calculated velocities at each pixel height with a variance of less than 1% (Hill et al. 2021). Mean velocity and normalized standard deviation profiles are shown in **Figure 12*d*** and **12*e***, respectively, for both the sharp-tip and blunt-tip models. The sharp tip exhibited a thinner boundary layer with significantly higher velocity fluctuations. Comparison of the measured profiles demonstrates the ability of FLEET to resolve differences in the flow resulting from slight changes to the model geometry and indicates that the technique is capable of measuring intricate flow features in challenging hypersonic environments.

5. CONCLUDING REMARKS

This review surveyed the maturation of the FLEET velocity measurement technique as it rapidly evolved from its invention at Princeton University to benchtop laboratory experiments and numerous applications in large-scale wind tunnel facilities within a single decade (2011–2021). The need for in situ—and particle-free—wind tunnel velocity measurements was established. MTV was shown to be a particle-free alternative to the commonly used LDV, PIV, PTV, and DGV methods, all of which require particles. FLEET was then compared with existing MTV techniques, and several advantages of FLEET were identified. These include the use of just a single laser beam, which originates from a commercially available, turnkey laser. Light from a single laser beam simply needs to be focused by a single lens or a pair of lenses to a line or a point, where it continues to emit detectable fluorescence for tens of microseconds. Several excitation schemes using different laser wavelengths were examined. A variety of types of intensified camera systems and detection strategies were described to measure fluorescence from moving, tagged molecules to determine velocity. The only gas needed for the measurement is N_2 (or air). For these reasons, the FLEET technique has been embraced by the measurement community as relatively easy to implement and widely applicable to wind tunnel facilities operating with air and N_2. Since the signal intensity is 10 times stronger in N_2 than in air, several of the best demonstration measurements have been in facilities that operate with pure N_2. Many important or unique facilities operate with pure N_2, and this review surveyed several FLEET measurements in these facilities. Examples of FLEET velocimetry in transonic and hypersonic facilities were presented. Most of the measurements showed accuracies and precisions on the order of 1% of the flow velocity. Now that FLEET has been implemented in many large-scale facilities, we anticipate numerous high-quality measurements in coming years. Some of the most promising advances for application of the technique in large-scale wind tunnels within the next few years include automated scanning of the FLEET signal, the writing of a FLEET grid rather than a point or line, multicamera imaging for multicomponent velocity estimation, and the simultaneous measurement of velocity and other flow parameters.

SUMMARY POINTS

1. Compared to other methods, femtosecond laser electronic excitation tagging (FLEET) is an easy-to-implement tool for off-body velocimetry.
2. FLEET is based on multiphoton excitation of molecules. A rate-limiting recombination step produces visible fluorescence that typically lasts for tens of microseconds, allowing for accurate and precise velocity measurements.

3. FLEET works in nitrogen gas (N_2), which is the most prevalent gas on earth and is present in most wind tunnel facilities. FLEET also works in air but the signal is 10 times higher in N_2 than in air.
4. Multiple simple experimental setups are available to measure one, two, or three velocity components by tracing tagged points, multiple points, lines, or multiple lines.
5. The main advantages of FLEET are that it is simple, resulting in ease of implementation; that no particles or seed gas are required; that visible (nonultraviolet) windows can be used; that measurements are nearly instantaneous (typically acquired in a few to 10 μs); that measurements can be acquired at kHz and higher repetition rates to resolve unsteady phenomena; and that the analysis of images to determine velocity is relatively straightforward.
6. The main disadvantages of FLEET include the fact that the laser and camera equipment are relatively expensive, the laser energy addition can locally heat the gas by tens to hundreds of degrees Celsius and can generate weak shock waves and acoustic waves that could perturb the flow, and the high-powered laser beams can damage windows or wind tunnel models. Furthermore, not all species exhibit the long-lived lifetimes needed for FLEET. To obtain 2D or 3D data, one needs to scan the measurement points or lines spatially around the flow, which can be time consuming. Increased precision comes at the cost of decreased spatial resolution.

FUTURE ISSUES

1. Even though FLEET is one of the easiest measurement techniques available, significant effort is still required to fully implement the technique in large-scale wind tunnels. The multiple, large-camera systems required for multiple-velocity-component measurements will be expensive and time consuming to implement, and these multiple-component systems must be engineered for reliability.
2. The acquisition of FLEET data over a spatial domain is relatively slow since measurements are typically at a point or a line. Automation of data acquisition, including traversing the laser focus and focusing the camera, will be required to improve operational efficiencies.
3. More sophisticated optical systems may be required to probe large fields of view or multiple locations in a flow field. Building infrastructure for such systems could be costly.
4. Creative measurement schemes may be required to measure velocities close to surfaces with FLEET since the laser energy is high enough to damage expensive wind tunnel models.
5. Since velocity is not the only parameter of interest in fluid mechanics, it would be advantageous for other parameters (density, pressure, temperature, and species composition) to be measured simultaneously with FLEET velocity.

DISCLOSURE STATEMENT

The authors are not aware of any biases that might be perceived as affecting the objectivity of this review.

ACKNOWLEDGMENTS

Funding for FLEET development at NASA Langley has mainly been provided by the NASA Langley Research Center's Internal Research and Development (IRAD) program, NASA's Center Innovation Fund (CIF), and NASA's Aerosciences Evaluation and Test Capabilities (AETC) portfolio. Sandia National Laboratories is a multimission laboratory managed and operated by National Technology and Engineering Solutions of Sandia, LLC, a wholly owned subsidiary of Honeywell International Inc., for the U.S. Department of Energy's National Nuclear Security Administration under contract DE-NA0003525.

LITERATURE CITED

Adelgren RG, Yan H, Elliott GS, Knight DD, Beutner TJ, Zheltovodov AA. 2005. Control of edney IV interaction by pulsed laser energy deposition. *AIAA J.* 43:256–69

Adrian RJ. 1991. Particle-imaging techniques for experimental fluid mechanics. *Annu. Rev. Fluid Mech.* 23:261–304

Bak MS, Wermer L, Im SK. 2015. Schlieren imaging investigation of successive laser-induced breakdowns in atmospheric-pressure air. *J. Phys. D* 48:485203

Balla RJ. 2013. Iodine tagging velocimetry in a Mach 10 wake. *AIAA J.* 51:1783–85

Beresh SJ, Casper KM, Wagner JL, Henfling JF, Spillers RW, Pruett BO. 2015. Modernization of Sandia's hypersonic wind tunnel. In *53rd AIAA Aerospace Sciences Meeting*. AIAA Pap. 2015-1338

Boguszko M, Elliott GS. 2005. On the use of filtered Rayleigh scattering for measurements in compressible flows and thermal fields. *Exp. Fluids* 38:33–49

Brieschenk S, O'Byrne S, Kleine H. 2013. Visualization of jet development in laser-induced plasmas. *Opt. Lett.* 38:664–66

Burns RA, Danehy PM. 2017. Unseeded velocity measurements around a transonic airfoil using femtosecond laser tagging. *AIAA J.* 55:4142–54

Burns RA, Danehy PM, Halls BR, Jiang N. 2015. *Application of FLEET velocimetry in the NASA langley 0.3-meter transonic cryogenic tunnel*. Paper presented at AIAA Aerodynamic Measurement Technology and Ground Testing Conference, 31st, Dallas, TX, AIAA Pap. 2015-2566

Burns RA, Danehy PM, Halls BR, Jiang N. 2017. Femtosecond laser electronic excitation tagging velocimetry in a transonic, cryogenic wind tunnel. *AIAA J.* 55:680–85

Burns RA, Danehy PM, Jiang N, Slipshenko MN, Felver J, Roy S. 2018a. Unseeded velocimetry in nitrogen for high-pressure, cryogenic wind tunnels, part II: picosecond-laser tagging. *Meas. Sci. Technol.* 29(11):115203

Burns RA, Danehy PM, Peters CJ. 2016. *Multiparameter flowfield measurements in high-pressure, cryogenic environments using femtosecond lasers*. Paper presented at AIAA Aerodynamic Measurement Technology and Ground Testing Conference, 32nd, Washington, DC, AIAA Pap. 2016-3246

Burns RA, Peters CJ, Danehy PM. 2018b. Unseeded velocimetry in nitrogen for high-pressure, cryogenic wind tunnels, part I: femtosecond-laser tagging. *Meas. Sci. Technol.* 29(11):115302

Cadel DR, Lowe KT. 2015. Cross-correlation Doppler global velocimetry (CC-DGV). *Opt. Lasers Eng.* 71:51–61

Calvert ND, Dogariu A, Miles RB. 2013. *FLEET boundary layer velocity profile measurements.* Paper presented at AIAA Plasmadynamics and Lasers Conference, 44th, San Diego, CA, AIAA Pap. 2013-2762

Calvert ND, Dogariu A, Miles RB. 2014. *2-D velocity and vorticity measurements with FLEET*. Paper presented at AIAA Aerodynamic Measurement Technology and Ground Testing Conference, 30th, Atlanta, GA, AIAA Pap. 2014-2229

Calvert ND, Zhang Y, Miles RB. 2016. *Characterizing FLEET for aerodynamic measurements in various gas mixtures and non-air environments*. Paper presented at AIAA Aerodynamic Measurement Technology and Ground Testing Conference, 32nd, Washington, DC, AIAA Pap. 2016-3206

Chin SL. 2009. *Femtosecond Laser Filamentation*. New York: Springer-Verlag

Chin SL, Wang TJ, Marceau C, Wu J, Liu JS, et al. 2012. Advances in intense femtosecond laser filamentation in air. *Laser Phys.* 22:1–53

Clark AM, Slotnick JP, Taylor N, Rumsey CL. 2020. *Requirements and challenges for CFD validation within the high-lift common research model ecosystem*. Paper presented at AIAA Aviation 2020 Forum, online, AIAA Pap. 2020-2772

Danehy PM, Bathel BF, Calvert N, Dogariu A, Miles RP. 2014. *Three-component velocity and acceleration measurement using FLEET*. Paper presented at AIAA Aerodynamic Measurement Technology and Ground Testing Conference, 30th, Atlanta, GA, AIAA Pap. 2014-2228

Danehy PM, Mere P, Gaston MJ, O'Byrne S, Palma PC, Houwing AF. 2001. Fluorescence velocimetry of the hypersonic, separated flow over a cone. *AIAA J.* 39:1320–28

Danehy PM, O'Byrne S, Houwing AFP, Fox JS, Smith DR. 2003. Flow-tagging velocimetry for hypersonic flows using fluorescence of nitric oxide. *AIAA J.* 41:263–71

Dedic CE, Cutler AD, Danehy PM. 2019. *Characterization of supersonic flows using hybrid fs/ps CARS*. Paper presented at AIAA Scitech 2019 Forum, San Diego, CA, AIAA Pap. 2019-1085

DeLuca NJ, Miles RB, Jiang N, Kulatilaka WD, Patnaik AK, Gord JR. 2017. FLEET velocimetry for combustion and flow diagnostics. *Appl. Opt.* 56:8632–38

DeLuca NJ, Miles RB, Kulatilakaz WD, Jiang N, Gord JR. 2014. *Femtosecond laser electronic excitation tagging (FLEET) fundamental pulse energy and spectral response*. Paper presented at AIAA Aerodynamic Measurement Technology and Ground Testing Conference, 30th, Atlanta, GA, AIAA Pap. 2014-2227

Dogariu A, Dogariu LE, Smith MS, McManamen B, Lafferty JF, Miles RB. 2021. *Velocity and temperature measurements in Mach 18 nitrogen flow at Tunnel 9*. Paper Presented at AIAA Scitech 2021 Forum, online, AIAA Pap. 2021-0020

Dogariu LE, Dogariu A, Miles RB, Smith MS, Marineau EC. 2019. Femtosecond laser electronic excitation tagging velocimetry in a large-scale hypersonic facility. *AIAA J.* 57:4725–37

Doll U, Stockhausen G, Willert C. 2017. Pressure, temperature, and three-component velocity fields by filtered Rayleigh scattering velocimetry. *Opt. Lett.* 42:3773–76

Edwards MR, Dogariu A, Miles RB. 2015a. Simultaneous temperature and velocity measurements in air with femtosecond laser tagging. *AIAA J.* 53:2280–88

Edwards MR, Limbach CM, Miles RB, Tropina AA. 2015b. *Limitations on high-spatial-resolution measurements of turbulence using femtosecond laser tagging*. Paper presented at AIAA Aerospace Sciences Meeting, 53rd, Kissimmee, FL, AIAA Pap. 2015-1219

Elias PQ, Severac N, Luyssen JM, Tobeli JP, Lambert F, et al. 2018. *Experimental investigation of linear energy deposition using femtosecond laser filamentation in a M=3 supersonic flow*. Paper presented at 2018 Joint Propulsion Conference, Cincinnati, OH, AIAA Pap. 2018-4896

Fisher JM, Braun J, Meyer TR, Paniagua G. 2020a. Application of femtosecond laser electronic excitation tagging (FLEET) velocimetry in a bladeless turbine. *Meas. Sci. Technol.* 31:064005

Fisher JM, Chynoweth BC, Smyser ME, Webb AM, Slipchenko MN, et al. 2021. Femtosecond laser electronic excitation tagging velocimetry in a Mach six quiet tunnel. *AIAA J.* 59:768–72

Fisher JM, Smyser ME, Slipchenko MN, Roy S, Meyer TR. 2020b. Burst-mode femtosecond laser electronic excitation tagging for kHz–MHz seedless velocimetry. *Opt. Lett.* 45:335–38

Forkey JN, Finkelstein ND, Lempert WR, Miles RB. 1996. Demonstration and characterization of filtered Rayleigh scattering for planar velocity measurements. *AIAA J.* 34:442–48

Gao Q, Zhang D, Li X, Li B, Li Z. 2019. Femtosecond-laser electronic-excitation tagging velocimetry using a 267 nm laser. *Sens. Actuators A* 287:138–42

Gendrich CP, Koochesfahani MM. 1996. A spatial correlation technique for estimating velocity fields using molecular tagging velocimetry (MTV). *Exp. Fluids* 22:67–77

Georgiadis NJ, Yoder DA, Vyas MA, Engblom WA. 2014. Status of turbulence modeling for hypersonic propulsion flowpaths. *Theor. Comput. Fluid Dyn.* 28:295–318

Glumac N, Elliott G, Boguszko M. 2005. Temporal and spatial evolution of a laser spark in air. *AIAA J.* 43:1984–94

Goodyer MJ. 1992. The cryogenic wind tunnel. *Prog. Aerosp. Sci.* 29:193–220

Grib SW, Stauffer HU, Roy S, Schumaker SA. 2021. Resonance-enhanced, rare-gas-assisted femtosecond-laser electronic-excitation tagging (FLEET) in argon/nitrogen mixture. *Appl. Opt.* 60:32–37

Halls BR, Jiang N, Gord JR, Danehy PM, Roy S. 2017. Mixture-fraction measurements with femtosecond-laser electronic-excitation tagging. *Appl. Opt.* 56:94–98

Hanson RK. 2011. Applications of quantitative laser sensors to kinetics, propulsion and practical energy systems. *Proc. Combust. Inst.* 33:1–40

Hill JL, Su PS, Jiang N, Grib SW, Roy S, et al. 2021. Hypersonic N_2 boundary-layer flow velocity profile measurements using FLEET. *Appl. Opt.* 60:38–46

Hiller B, Booman RA, Hassa C, Hanson RK. 1984. Velocity visualization in gas flows using laser-induced phosphorescence of biacetyl. *Rev. Sci. Instrum.* 55:1964–67

Hsu PS, Jiang N, Danehy P, Gord J, Roy S. 2018a. Fiber-coupled ultrashort-pulse-laser-based electronic-excitation tagging velocimetry. *Appl. Opt.* 57:560–66

Hsu PS, Jiang N, Jewell J, Felver J, Borg M, et al. 2020. 100 kHz PLEET velocimetry in a Mach-6 Ludwieg tube. *Opt. Express* 28:21982

Hsu PS, Patnaik AK, Stolt AJ, Estevadeordal J, Roy S, Gord JR. 2018b. Femtosecond-laser-induced plasma spectroscopy for high-pressure gas sensing: enhanced stability of spectroscopic signal. *Appl. Phys. Lett.* 113:214103

Huffman RE, Elliott GS. 2009. *An experimental investigation of accurate particle tracking in supersonic, rarefied axisymmetric jets*. Paper presented at AIAA Aerospace Sciences Meeting, 47th, Orlando, FL, AIAA Pap. 2009-1265

Jiang N, Halls BR, Stauffer HU, Danehy PM, Gord JR, Roy S. 2016. Selective two-photon absorptive resonance femtosecond-laser electronic-excitation tagging velocimetry. *Opt. Lett.* 41:2225–28

Jiang N, Mance JG, Slipchenko MN, Felver JJ, Stauffer HU, et al. 2017. Seedless velocimetry at 100 kHz with picosecond-laser electronic-excitation tagging. *Opt. Lett.* 42:239–42

Kandala R, Candled GV. 2004. Numerical studies of laser-induced energy deposition for supersonic flow control. *AIAA J.* 42:2266–75

Kearney SP, Richardson DR, Retter JE, Dedic CE, Danehy PM. 2020 *Simultaneous temperature/pressure monitoring in compressible flows using hybrid fs/ps pure-rotational CARS*. Paper presented at AIAA Scitech 2020 Forum, Orlando, FL, AIAA Pap. 2020-0770

Klavuhn KG, Gauba G, McDaniel JC. 1994. OH laser-induced fluorescence velocimetry technique for steady, high-speed, reacting flows. *J. Propuls. Power* 10:787–97

Knight D. 2008. Survey of aerodynamic drag reduction at high speed by energy deposition. *J. Propuls. Power* 24:1153–67

Koochesfahani MM, Nocera DG. 2007. Molecular tagging velocimetry. In *Handbook of Experimenal Fluid Dynamics*, ed. J Foss, C Tropea, A Yarin, pp. 362–82. Berlin: Springer-Verlag

Laux CO. 2002. Radiation and nonequilibrium collisional-radiative models. In *Physico-Chemical Models of High Enthalpy and Plasma Flows*, ed. D Fletcher, T Magin, JM Charbonnier, GSR Sarma. Rhode-Saint-Genèse, Belg.: Von Karman Inst. Fluid Dyn.

Lempert WR, Jiang N, Sethuram S, Samimy M. 2002. Molecular tagging velocimetry measurements in supersonic microjets. *AIAA J.* 40:1065–70

Lempert WR, Ronney P, Magee K, Gee KR, Haugland RP. 1995. Flow tagging velocimetry in incompressible flow using photo-activated nonintrusive tracking of molecular motion (PHANTOMM). *Exp. Fluids* 18:249–57

Li B, Tian Y, Gao Q, Zhang D, Li X, et al. 2018. Filamentary anemometry using femtosecond laser-extended electric discharge—FALED. *Opt. Express* 26:21132–40

Li B, Zhang D, Liu J, Tian Y, Gao Q, Li Z. 2019. A review of femtosecond laser-induced emission techniques for combustion and flow field diagnostics. *Appl. Sci.* 9(9):1906

Limbach C. 2015. *Characterization of nanosecond, femtosecond and dual pulse laser energy deposition in air for flow control and diagnostic applications*. PhD Thesis, Princeton Univ., Princeton, NJ

Limbach CM, Miles RB. 2017. Rayleigh scattering measurements of heating and gas perturbations accompanying femtosecond laser tagging. *AIAA J.* 55:112–20

Loth E. 2008. Compressibility and rarefaction effects on drag of a spherical particle. *AIAA J.* 46:2219–28

Marshall GJ, Zhang Y, Beresh SJ, Richardson DR, Casper KM. 2021. *Developing multi-line FLEET using periodic mask design*. Paper presented at AIAA Scitech 2021 Forum, online, AIAA Pap. 2021-0021

McDaniel JC, Hiller B, Hanson RK. 1983. Simultaneous multiple-point velocity measurements using laser-induced iodine fluorescence. *Opt. Lett.* 8:51–53

Melling A. 1997. Tracer particles and seeding for particle image velocimetry. *Meas. Sci. Technol.* 8:1406–16
Michael JB, Edwards MR, Dogariu A, Miles RB. 2011. Femtosecond laser electronic excitation tagging for quantitative velocity imaging in air. *Appl. Opt.* 50:5158–62
Michael JB, Edwards MR, Dogariu A, Miles RB. 2012. *Velocimetry by femtosecond laser electronic excitation tagging (FLEET) of air and nitrogen*. Paper presented at AIAA Aerospace Sciences Meeting, 50th, Nashville, TN, AIAA Pap. 2021-1053
Miles RB, Cohen C, Connors J, Howard P, Huang S, et al. 1987. Velocity measurements by vibrational tagging and fluorescent probing of oxygen. *Opt. Lett.* 12:861–63
Miles RB, Dogariu A, Michael JB, Edwards MR. 2018. *Femtosecond laser excitation tagging anemometry*. US Patent 9,863,975 B2
Miles RB, Lempert WR. 1997. Quantitative flow visualization in unseeded flows. *Annu. Rev. Fluid Mech.* 29:285–326
Miles RB, Michael JB, Limbach CM, McGuire SD, Chng TL, et al. 2015. New diagnostic methods for laser plasma- and microwave-enhanced combustion. *Philos. Trans. R. Soc. A* 373:20140338
Mills JL, Sukenik CI, Balla RJ. 2011. *Hypersonic wake diagnostics using laser induced fluorescence techniques*. Paper presented at AIAA Plasmadynamics and Lasers Conference, 42nd, Honolulu, HI, AIAA Pap. 2011-3459
Nishihara M, Freund JB, Elliott GS. 2020. A study of velocity, temperature, and density in the plasma generated by laser-induced breakdowns. *J. Phys. D* 53:105203
Osuka T, Erdem E, Hasegawa N, Majima R, Tamba T, et al. 2014. Laser energy deposition effectiveness on shock-wave boundary-layer interactions over cylinder-flare combinations. *Phys. Fluids* 26:096103
Parziale NJ, Smith MS, Marineau EC. 2015. Krypton tagging velocimetry of an underexpanded jet. *Appl. Opt.* 54:5094–101
Peters CJ. 2019. *Considerations for femtosecond laser electronic excitation tagging in high-speed flows*. PhD Thesis, Princeton Univ., Princeton, NJ
Peters CJ, Burns RA, Miles RB, Danehy PM. 2020. Effect of low temperatures and pressures on signal, lifetime, accuracy and precision of femtosecond laser tagging velocimetry. *Meas. Sci. Technol.* 32:035202
Peters CJ, Danehy PM, Bathel BF, Jiang N, Calvert ND, Miles RB. 2015. *Precision of FLEET velocimetry using high-speed CMOS camera systems*. Paper presented at AIAA Aerodynamic Measurement Technology and Ground Testing Conference, 31st, Dallas, TX, AIAA Pap. 2015-2565
Peters CJ, Miles RB, Burns RA, Bathel BF, Jones GS, Danehy PM. 2016. *Femtosecond laser tagging characterization of a sweeping jet actuator operating in the compressible regime*. Paper presented at AIAA Aerodynamic Measurement Technology and Ground Testing Conference, 32nd, Washington, DC, AIAA Pap. 2016-3248
Pitz RW, Wehrmeyer JA, Ribarov LA, Oguss DA, Batliwala F, et al. 2000. Unseeded molecular flow tagging in cold and hot flows using ozone and hydroxyl tagging velocimetry. *Meas. Sci. Technol.* 11:1259–71
Pouya S, Van Rhijn A, Dantus M, Koochesfahani M. 2014. Multi-photon molecular tagging velocimetry with femtosecond excitation (FemtoMTV). *Exp. Fluids* 55:1791
Reese DT, Burns RA, Danehy PM, Walker E, Goad W. 2019a. *Implementation of a pulsed-laser measurement system in the National Transonic Facility*. Paper presented at AIAA Aviation 2019 Forum, Dallas, TX, AIAA Pap. 2019-3380
Reese DT, Danehy P, Jiang N, Felver J, Richardson D, Gord J. 2019b. Application of resonant femtosecond tagging velocimetry in the 0.3-meter transonic cryogenic tunnel. *AIAA J.* 57:3851–58
Reese DT, Jiang N, Danehy P. 2020. Unseeded velocimetry in nitrogen for high-pressure, cryogenic wind tunnels: part III. Resonant femtosecond-laser tagging. *Meas. Sci. Technol.* 31:075203
Reese DT, Thompson RJ, Burns RA, Danehy PM. 2021. Application of femtosecond-laser tagging for unseeded velocimetry in a large-scale transonic cryogenic wind tunnel. *Exp. Fluids* 62:99
Ribarov LA, Wehrmeyer JA, Pitz RW, Yetter RA. 2002. Hydroxyl tagging velocimetry (HTV) in experimental air flows. *Appl. Phys. B* 74:175–83
Ryabtsev A, Pouya S, Koochesfahani M, Dantus M. 2014. Vortices in the wake of a femtosecond laser filament. *Opt. Express* 22:26098–102
Sánchez-González R, Srinivasan R, Bowersox RDW, North SW. 2011. Simultaneous velocity and temperature measurements in gaseous flow fields using the VENOM technique. *Opt. Lett.* 36:196–98

Sijtsema NM, Dam NJ, Klein-Douwel RJ, Ter Meulen JJ. 2002. Air photolysis and recombination tracking: a new molecular tagging velocimetry scheme. *AIAA J.* 40:1061–64

Slotnick J, Khodadoust A, Alonso J, Darmofal D. 2014. *CFD Vision 2030 Study: a path to revolutionary computational aerosciences.* Contract. Rep. CR-2014-218178, NASA Langley Res. Cent., Hampton, VA

Talebpour A, Abdel-Fattah M, Bandrauk AD, Chin SL. 2001. Spectroscopy of the gases interacting with intense femtosecond laser pulses. *Laser Phys.* 11:68–76

Vassberg JC, DeHaan MA, Rivers SM, Wahls RA. 2008. *Development of a common research model for applied CFD validation studies*. Paper presented at AIAA Applied Aerodynamics Conference, 26th, Honolulu, HI, AIAA Pap. 2008-6919

Wahls RA. 2001. *The National Transonic Facility: a research retrospective*. Paper presented at Aerospace Sciences Meeting and Exhibit, 39th, Reno, NV, AIAA Pap. 2001-0754

Wang JM, Buchta DA, Freund JB. 2020. Hydrodynamic ejection caused by laser-induced optical breakdown. *J. Fluid Mech.* 888:A16

Westerweel J, Elsinga GE, Adrian RJ. 2013. Particle image velocimetry for complex and turbulent flows. *Annu. Rev. Fluid Mech.* 45:409–36

Williams OJ, Nguyen T, Schreyer AM, Smits AJ. 2015. Particle response analysis for particle image velocimetry in supersonic flows. *Phys. Fluids* 27:076101

Xu HL, Azarm A, Bernhardt J, Kamali Y, Chin SL. 2009. The mechanism of nitrogen fluorescence inside a femtosecond laser filament in air. *Chem. Phys.* 360:171–75

Yu X, Peng J, Sun R, Yang X, Wang C, et al. 2012. Stabilization of a premixed $CH_4/O_2/N_2$ flame using femtosecond laser-induced plasma. *Opt. Lett.* 37:2106–8

Yu X, Peng J, Yang P, Sun R, Yi Y, et al. 2010. Enhancement of a laminar premixed methane/oxygen/nitrogen flame speed using femtosecond-laser-induced plasma. *Appl. Phys. Lett.* 97:2008–11

Zhang D, Li B, Gao Q, Li Z. 2018. Applicability of femtosecond laser electronic excitation tagging in combustion flow field velocity measurements. *Appl. Spectrosc.* 72:1807–13

Zhang Y. 2018. *The development and characterization of femtosecond laser velocimetry methods*. PhD Thesis, Princeton Univ., Princeton, NJ

Zhang Y, Beresh SJ, Casper KM, Richardson DR, Soehnel M, Spillers R. 2020a. *Tailoring FLEET for cold hypersonic flows*. Paper presented at AIAA Scitech 2020 Forum, Orlando, FL, AIAA Pap. 2020-1020

Zhang Y, Calvert N, Dogariu A, Miles RB. 2016. *Towards shear flow measurements using FLEET*. Paper presented at AIAA Aerospace Sciences Meeting, 54th, San Diego, CA, AIAA Pap. 2016-0028

Zhang Y, Danehy PM, Miles RB. 2019a. Femtosecond laser tagging in R134a with small quantities of air. *AIAA J.* 57:1793–800

Zhang Y, Marshall G, Beresh S, Richardson D, Casper K. 2020b. Multi-line FLEET by imaging periodic masks. *Opt. Lett.* 45:3949–52

Zhang Y, Miles RB. 2017. *Characterizing the accuracy of FLEET velocimetry using comparison with hot wire anemometry*. Paper presented at AIAA Aerospace Sciences Meeting, 55th, Grapevine, TX, AIAA Pap. 2017-0256

Zhang Y, Miles RB. 2018a. Femtosecond laser tagging for velocimetry in argon and nitrogen gas mixtures. *Opt. Lett.* 43:551–54

Zhang Y, Miles RB. 2018b. *Shear layer measurements along curved surfaces using the FLEET method*. Paper presented at 2018 AIAA Aerospace Sciences Meeting, Kissimmee, FL, AIAA Pap. 2018-1768

Zhang Y, Richardson DR, Beresh SJ, Casper KM, Soehnel M, et al. 2019b. *Hypersonic wake measurements behind a slender cone using FLEET velocimetry*. Paper presented at AIAA Aviation 2019 Forum, Dallas, TX, AIAA Pap. 2019-3381

Annual Review of Fluid Mechanics

Volume 54, 2022

Contents

Indexes

Errata

An online log of corrections to *Annual Review of Fluid Mechanics* articles may be found at http://www.annualreviews.org/errata/fluid